1521-0111/12/8102-250–263$25.00
MOLECULAR PHARMACOLOGY
Vol. 81, No. 2
74013/3743995

Mol Pharmacol 81:250–263, 2012

Functional Selectivity in CB_2 Cannabinoid Receptor Signaling and Regulation: Implications for the Therapeutic Potential of CB_2 Ligands[S]

Brady K. Atwood, James Wager-Miller, Christopher Haskins, Alex Straiker, and Ken Mackie

Department of Psychological and Brain Sciences, Gill Center for Biomolecular Science, Indiana University, Bloomington, Indiana (B.K.A., J.W.-M., C.H., A.S., K.M.)

Received June 8, 2011; accepted November 7, 2011

ABSTRACT

Receptor internalization increases the flexibility and scope of G protein-coupled receptor (GPCR) signaling. CB_1 and CB_2 cannabinoid receptors undergo internalization after sustained exposure to agonists. However, it is not known whether different agonists internalize CB_2 to different extents. Because CB_2 is a promising therapeutic target, understanding its trafficking in response to different agonists is necessary for a complete understanding of its biology. Here we profile a number of cannabinoid receptor ligands and provide evidence for marked functional selectivity of cannabinoid receptor internalization. Classic, aminoalkylindole, bicyclic, cannabilactone, iminothiazole cannabinoid, and endocannabinoid ligands varied greatly in their effects on CB_1 and CB_2 trafficking. Our most striking finding was that (*R*)-(+)-[2,3-dihydro-5-methyl-3-(4-morpholinylmethyl) pyrrolo-[1,2,3-*d*,*e*]-1,4-benzoxazin-6-yl]-1-naphthalenyl-methanone (WIN55,212-2) (and other aminoalkylindoles) failed to promote CB_2 receptor internalization, whereas 5-(1,1-dimethylheptyl)-2-(5-hydroxy-2-(3-hydroxypropyl)cyclohexyl)phenol (CP55,940) robustly internalized CB_2 receptors. Furthermore, WIN55,212-2 competitively antagonized CP55,940-induced CB_2 internalization. Despite these differences in internalization, both compounds activated CB_2 receptors as measured by extracellular signal-regulated kinase 1/2 phosphorylation and recruitment of β-arrestin$_2$ to the membrane. In contrast, whereas CP55,940 inhibited voltage-gated calcium channels via CB_2 receptor activation, WIN55,212-2 was ineffective on its own and antagonized the effects of CP55,940. On the basis of the differences we found between these two ligands, we also tested the effects of other cannabinoids on these signaling pathways and found additional evidence for functional selectivity of CB_2 ligands. These novel data highlight that WIN55,212-2 and other cannabinoids show strong functional selectivity at CB_2 receptors and suggest that different classes of CB_2 ligands may produce diverse physiological effects, emphasizing that each class needs to be separately evaluated for therapeutic efficacy.

Introduction

Cannabinoid receptors are the targets of both endogenous cannabinoids (endocannabinoids) as well as exogenous cannabinoids such as Δ^9-tetrahydrocannabinol (THC) (Howlett et al., 2002). The CB_1 cannabinoid receptor is abundant within the brain (Mackie, 2005), whereas the CB_2 cannabinoid receptor is localized primarily in immune cells of both the periphery and the central nervous system. It is possible that it may be expressed in neurons, but the extent and level of expression remain controversial (Atwood and Mackie, 2010). Both CB_1 and CB_2 are GPCRs that couple to the $G_{i/o}$ class of G proteins. As such, they negatively couple to adenylyl cyclase, and both are capable of activating p42/44 MAPK (ERK1/2) (Felder et al., 1995; Howlett et al., 2002).

The CB_2 cannabinoid receptor is an attractive therapeutic target. CB_2 activation is immunomodulatory and neuroprotective (Berdyshev, 2000; Howlett et al., 2002; Cabral and Griffin-Thomas, 2009). CB_2 agonists also suppress both acute and neuropathic pain responses (Anand et al., 2009). CB_1 probably mediates most, if not all, of the psychoactive effects of cannabinoids (Huestis et al., 2001; Mackie, 2005; Monory et al., 2007), so CB_2-selective agonists are attractive as therapeutics because they would presumably lack this psychoactivity. CB_2 expression also increases under certain conditions and disease states, further adding to its attractiveness as a therapeutic target (Zhang et al., 2003; Wotherspoon et al., 2005; Yiangou et al., 2006).

However, CB_2 agonist-based therapies for many indications will necessitate long-term treatment. Long-term treatment with a GPCR agonist produces a number of physiological adap-

This work was supported by the National Institutes of Health National Institute on Drug Abuse [Grants DA011322, DA021696, DA009158]; and the National Institutes of Health National Institute for Research Resources [Grant RR025761].

Article, publication date, and citation information can be found at http://molpharm.aspetjournals.org.

http://dx.doi.org/10.1124/mol.111.074013.

[S] The online version of this article (available at http://molpharm.aspetjournals.org) contains supplemental material.

tations at both the systems and cellular levels. For instance, repeated morphine administration produces profound physiological tolerance (von Zastrow et al., 2003). At the cellular level, this prolonged exposure results in μ-opioid receptor desensitization (Koch et al., 2005), a functional decoupling of the receptor from its G proteins. Extended exposure to opioids also produces μ-opioid receptor internalization (Koch et al., 2005). It has been suggested that there is an inverse relationship between μ-opioid receptor internalization and desensitization (Whistler et al., 1999; Finn and Whistler, 2001; Koch et al., 2005; Koch and Höllt, 2008). This may also be true for CB_1 cannabinoid receptors. (*R*)-(+)-[2,3-Dihydro-5-methyl-3-(4-morpholinylmethyl) pyrrolo-[1,2,3-*d*,*e*]-1,4-benzoxazin-6-yl]-1-naphthalenyl-methanone (WIN55,212-2) is a cannabinoid receptor agonist that produces substantial CB_1 internalization (Hsieh et al., 1999) but less receptor desensitization than THC, an agonist that produces low receptor internalization (Wu et al., 2008).

Little is known about CB_2 receptor internalization. There is evidence from expression systems that CB_2 undergoes constitutive activation resulting in a basal level of internalization. A CB_2 agonist, 5-(1,1-dimethylheptyl)-2-(5-hydroxy-2-(3-hydroxypropyl)cyclohexyl)phenol (CP55,940), enhances internalization, whereas *N*-((1*S*)-endo-1,3,3-trimethyl bicyclo heptan-2-yl)-5-(4-chloro-3-methylphenyl)-1-(4-methylbenzyl)-pyrazole-3-carboxamide) (SR144528), a CB_2 receptor inverse agonist, prevents it, increasing cell surface CB_2 (Bouaboula et al., 1999). A recent study found that [(1*R*,2*R*,5*R*)-2-[2,6-dimethoxy-4-(2-methyloctan-2-yl)phenyl]-7,7-dimethyl-4-bicyclo[3.1.1]hept-3-enyl] methanol (HU-308) promotes CB_2 internalization and this internalization can be reversed by iodopravadoline (AM630). This study also found that AM630 acted as an inverse agonist with regard to internalization (Grimsey et al., 2011). If CB_2 agonists will be used therapeutically, then a greater understanding of the cellular compensations that occur during lengthy drug treatments will be necessary. Here we characterized a selection of distinct cannabinoid ligands from a number of different structural classes to determine their ability to internalize CB_2 receptors. We hypothesized that potent and efficacious CB_2 agonists would produce greater amounts of internalization than those of lower potency and efficacy. Furthermore, we expected that ligands that were highly selective for CB_2 over CB_1 would produce greater internalization of CB_2 than CB_1.

Our investigation of CB_2 receptor internalization, led us to explore the functional selectivity of CP55,940 and WIN55,212-2, two of the most frequently used cannabinoid agonists, at CB_2. Functional selectivity is an important emerging pharmacological concept that describes the ability of different receptor ligands to produce distinct cellular responses that are due to the activation of differing repertoires of signaling pathways (Urban et al., 2007). There is evidence that some CB_2 agonists display functional selectivity (Shoemaker et al., 2005). In addition to measuring internalization due to CP55,940 and WIN55,212-2, we also measured CB_2-mediated MAPK activation, β-arrestin$_2$ membrane recruitment, and inhibition of voltage-gated calcium channels. These studies found that although CP55,940 was an efficacious agonist for all signaling pathways studied, WIN55,212-2 displayed profound functional selectivity, activating only a few of these signaling pathways. In addition to WIN55,212-2, we found that several other CB_2 agonists exhibited significant functional selectivity in these cellular signaling pathways.

Materials and Methods

Reagents. Drugs and reagents were purchased from Tocris Cookson (Ellisville, MO), Cayman Chemical (Ann Arbor, MI), Invitrogen (Carlsbad, CA), Thermo Fisher Scientific (Waltham, MA), LI-COR Biosciences (Lincoln, NE), Clontech (Mountain View, CA), or Sigma-Aldrich (St. Louis, MO). Naphthalen-1-yl-(1-pentylindol-3-yl)methanone (JWH018) was synthesized as described in (Huffman et al., 1994). CP55,940, rimonabant (SR141716), *N*-[(1*S*)-endo-1,3,3-trimethylbicyclo [2.2.1]heptan2-yl]-5-(4-chloro-3-methylphenyl)-1-[(4-methylphenyl)methyl]-1*H*-pyrazole-3-carboxamide (SR144528), and THC were obtained from the National Institute of Drug Abuse Drug Supply Service. *N*-[3-(2-Methoxyethyl)-4,5-dimethyl-1,3-thiazol-2-ylidene]-2,2,3,3-tetramethylcyclopropane-1-carboxamide (A-836339) was generously provided by Abbott Laboratories (Abbott Park, IL), 3-(1,1-dimethyl-heptyl)-1-hydroxy-9-methoxy-benzo(*c*)chromen-6-one (AM1710) was from Andrea Hohmann (Indiana University, Bloomington, IN), and Δ^8-tetrahydrocannabinol dimethyl heptyl (HU210) was from Dr. Raphael Mechoulam (Hebrew University, Jerusalem, Israel). 2-[(1*R*,3*S*)-3-Hydroxycyclohexyl]- 5-(2-methyloctan-2-yl)phenol (CP47,497) C8 homolog was synthesized as described by Atwood et al. (2011). THCV was obtained from Aron Lichtman (Virginia Commonwealth University, Richmond, VA).

Mouse anti-HA11 antibody was purchased from Covance (Richmond, CA). Rabbit anti-phospho-ERK1/2 MAPK was purchased from Cell Signaling Technologies Inc. (Danvers, MA). IRDye conjugated goat anti-mouse IgG antibody was purchased from LI-COR Biosciences (Lincoln, NE). Donkey anti-rabbit IgG IR800 antibody was purchased from Rockland Immunochemicals Inc. (Gilbertsville, PA). Fluorescein isothiocyanate-conjugated secondary antibody was purchased from Jackson ImmunoResearch Laboratories Inc. (West

ABBREVIATIONS: 2-AG, 2-arachidonoylglycerol; A-836339, *N*-[3-(2-methoxyethyl)-4,5-dimethyl-1,3-thiazol-2-ylidene]-2,2,3,3-tetramethylcyclopropane-1-carboxamide; AEA, anandamide; AM1241, (2-iodo-5-nitrophenyl)-[1-[(1-methylpiperidin-2-yl)methyl]indol-3-yl]methanone; AM1710, 3-(1,1-dimethyl-heptyl)-1-hydroxy-9-methoxy-benzo(c)chromen-6-one; AM630, iodopravadoline; BSA, bovine serum albumin; CB_1, cannabinoid receptor subtype 1; CB_2, cannabinoid receptor subtype 2; CP47,497, 2-[(1*R*,3*S*)-3-hydroxycyclohexyl]- 5-(2-methyloctan-2-yl)phenol; CP55,940, 5-(1,1-dimethylheptyl)-2-(5-hydroxy-2-(3-hydroxypropyl)cyclohexyl)phenol; ECS, extracellular solution; ERK, extracellular signal-regulated kinase; FAAH, fatty acid amide hydrolase; GPCR, G-protein-coupled receptor; GW405833, 1-(2,3-dichlorobenzoyl)-5-methoxy-2-methyl-3-[2-(4-morpholinyl)ethyl]-1*H*-indole; HA, hemagglutinin 11; HBS, HEPES-buffered saline; h, human; HEK, human embryonic kidney; HU-210, Δ^8-tetrahydrocannabinol dimethyl heptyl; HU-308, [(1*R*,2*R*,5*R*)-2-[2,6-dimethoxy-4-(2-methyloctan-2-yl)phenyl]-7,7-dimethyl-4-bicyclo[3.1.1]hept-3-enyl] methanol; JWH015, (2-methyl-1-propyl-1*H*-indol-3-yl)-1-naphthalenylmethanone; JWH018, naphthalen-1-yl-(1-pentylindol-3-yl)methanone; JWH133, (6*aR*,10*aR*)-3-(1,1-dimethylbutyl)-6*a*,7,10,10*a*-tetrahydro -6,6,9-trimethyl-6*H*-dibenzo[*b*,*d*]pyran; JZL184, 4-nitrophenyl-4-[bis(1,3-benzodioxol-5-yl)(hydroxy)methyl]piperidine-1-carboxylate; m, mouse; MAPK, mitogen-activated protein kinase; MGL, monoacylglycerol lipase; mRFP, modified red fluorescent protein; PBS, phosphate-buffered saline; PFA, paraformaldehyde; pplss, preprolactin signal sequence; PTX, pertussis toxin; r, rat; SR141716, rimonabant; SR144528, *N*-((1*S*)-endo-1,3,3-trimethyl bicyclo heptan-2-yl)-5-(4-chloro-3-methylphenyl)-1-(4-methylbenzyl)-pyrazole-3-carboxamide); SR144528, *N*-[(1*S*)-endo-1,3,3-trimethylbicyclo [2.2.1]heptan2-yl]-5-(4-chloro-3-methylphenyl)-1-[(4-methylphenyl)methyl]-1*H*-pyrazole-3-carboxamide; TBS, Tris-buffered saline; THC, Δ^9-tetrahydrocannabinol; THCV, tetrahydrocannabivarin; URB597, [3-(3-carbamoylphenyl)phenyl] *N*-cyclohexylcarbamate; VGCC, voltage-gated calcium channel; WIN55,212-2, (*R*)-(+)-[2,3-dihydro-5-methyl-3-(4-morpholinylmethyl) pyrrolo-[1,2,3-*d*,*e*]-1,4-benzoxazin-6-yl]-1-naphthalenyl-methanone.

Grove, PA). Vectashield mounting medium was purchased from Vector Laboratories (Burlingame, CA). The anti-N-terminal human CB_2 antibody was previously characterized (Benito et al., 2005).

Solutions used in immunocytochemistry, MAPK, and internalization assays included phosphate buffer (100 mM NaH_2PO_4, pH 7.4), phosphate-buffered saline (PBS; 137 mM NaCl, 100 mM NaH_2PO_4, and 2.7 mM KCl, pH 7.4), HEPES-buffered saline (HBS; 130 mM NaCl, 5.4 mM KCl, 1.8 mM $MgCl_2$, and 10 mM HEPES, pH 7.5), Tris-buffered saline (TBS; 137 mM NaCl and 10 mM Tris, pH 7.4), and 4% paraformaldehyde [4% PFA (w/v) in phosphate buffer].

For electrophysiological recordings, normal extracellular solution (ECS) contained 119 mM NaCl, 5 mM KCl, 2 mM $CaCl_2$, 1 mM $MgCl_2$, 30 mM glucose, and 20 mM HEPES, pH adjusted to 7.3 with NaOH. For recording barium currents, the ECS contained 119 mM NaCl, 5 mM KCl, 10 mM $BaCl_2$, 1 mM $MgCl_2$, 30 mM glucose, and 20 mM HEPES, pH adjusted to 7.3 with NaOH. To block sodium currents during calcium channel recordings, >200 nM tetrodotoxin was added to the ECS. Nifedipine (10 μM) was also added to block L-type calcium channels. The intracellular solution for recording calcium currents contained 100 mM CsCl, 1 mM $MgCl_2$, 3 mM MgATP, 0.3 mM LiGTP, 10 mM HEPES, 20 mM phosphocreatine, 10 mM EGTA, and 50 units/ml creatine phosphokinase, pH adjusted to 7.3 with CsOH.

Cell Culture. HEK and AtT20 cells were purchased from the American Type Culture Collection (Manassas, VA). AtT20 cells used for calcium channel recordings were generously provided by Dr. Gerry Oxford (Indiana University School of Medicine, Indianapolis, IN). AtT20 cell transfection was performed using the Superfect reagent (QIAGEN, Valencia, CA). HEK293 cell transfection was done using the Lipofectamine 2000 reagent (Invitrogen, Carlsbad, CA). Both were conducted according to the manufacturer's instructions. Stable cell lines were made as described previously (Brown et al., 2002; Daigle et al., 2008). Plasmids encoding pplss-HA-rat CB_1-pcDNA3.0 (rCB_1), pplss-HA-mouse CB_2-pcDNA3.0 (mCB_2), HA-rat CB_2-pcDNA3.0 (rCB_2), pplss-HA-human CB_2-pTRE2 (hCB_2), human CB_2-pcDNA3 (untagged hCB_2), and β-$arrestin_2$-mRFP pEF4a were all constructed, amplified, and purified using New England BioLabs (Ipswich, MA) buffers and restriction enzymes and QIAGEN (Valencia, CA) plasmid DNA purification kits according to the manufacturer's instructions. The amino-terminal HA (hemagglutinin) epitope tag was added for ease of immunostaining. An amino-terminal preprolactin signal sequence (pplss) was added to enhance cannabinoid receptor surface expression in HEK293 cells (Daigle et al., 2008). The pTRE2 vector was chosen for hCB_2 because of the extremely higher expression levels obtained using hCB_2 in the pcDNA3.0 plasmid. Sequencing was performed to verify each construct's integrity (Indiana University Molecular Biology Institute). Primers for sequencing and cloning were purchased from Operon (Huntsville, AL). Cell lines were grown in Dulbecco's modified Eagle's medium with 10% fetal bovine serum, 100 units/ml penicillin, and 100 μg/ml streptomycin. All cells were grown at 37°C in 5% CO_2 humidified air.

Immunocytochemistry. HEK293 cells expressing rCB_1 and rCB_2 were treated and immunostained according to the protocols outlined in Daigle et al. (2008) and Kearn et al. (2005). In brief, cells were grown on poly(D-lysine)-coated coverslips in 24-well plates. Cells were washed once with HBS/BSA (HBS + 0.2 mg/ml BSA) and drug treatments were performed at 37°C with drugs diluted in HBS/BSA. After drug treatments, cells were fixed with 4% paraformaldehyde, washed, and blocked in PBS with 5% donkey serum and 0.1% saponin (for membrane permeabilization). Primary antibody treatment was performed for 3 h at room temperature or overnight at 4°C. Cells were washed and secondary antibody incubation was done for 1 h at room temperature. Finally, cells were washed, dried, and mounted on glass slides using Vectashield with 4,6-diamidino-2-phenylindole. Cells were visualized using a Nikon Eclipse TE2000E confocal microscope at 60× magnification for internalization experiments and 100× for β-arrestin experiments (Indiana University METACyt facilities).

Internalization and MAPK Assays. Internalization assays (quantitative on-cell Western blot) were performed as described previously in Atwood et al. (2010). For internalization experiments using pertussis toxin (PTX), the cells were incubated overnight in PTX (400 ng/ml). For internalization experiments using sucrose (350 mM), [3-(3-carbamoylphenyl)phenyl] *N*-cyclohexylcarbamate (URB597; 100 nM), and 4-nitrophenyl-4-[bis(1,3-benzodioxol-5-yl)(hydroxy)methyl]piperidine-1-carboxylate (JZL184; 100 nM), the cells were pretreated for 20 min and the treatment was continued throughout the duration of the experiment. For experiments comparing untagged to HA-tagged receptors, an anti-N-terminal rat CB_2 antibody was used instead of the anti-HA antibody used in all other experiments. At least three replicates for each time point or concentration were performed for each independent experiment.

For MAPK assays (quantitative in-cell system), HEK293 cells stably expressing rCB_1 or rCB_2 were plated to near confluence on poly(D-lysine)-coated 96-well plates (Corning Life Sciences, Lowell, MA) in serum-free growth media and incubated overnight. Drug-containing solutions were made in the serum-free media and added to the wells at appropriate time points. After drug incubation, the wells were emptied and ice-cold 4% PFA was added immediately to each well and the plates were placed on ice for 15 min, followed by 30 min at room temperature. The PFA was then removed, and >100 μl of ice-cold methanol was added to each well, and the plate was incubated at −20°C for >15 min. An additional washing step was performed using PBS containing 0.1% Triton X-100 for 25 min (five 5-min washes). The PBS/Triton X-100 was replaced with Odyssey blocking buffer and incubated for >1.5 h at room temperature. The blocking solution was then removed and replaced by blocking solution containing rabbit anti-phospho-ERK1/2 MAPK antibody (1:200) and was shaken overnight at 4°C or for 2.5 h at room temperature. The antibody solution was removed, and the plates were washed five times with TBS containing 0.05% Tween 20 for 5 min each time. Blocking solution containing a donkey anti-rabbit IgG antibody (1:200 dilution) conjugated with an IR800 dye was added and shaken for 1 h at room temperature. The plates were then washed five times with TBS containing 0.05% Tween 20, 5 min each time. The plates were patted dry and then scanned using a LI-COR Odyssey. The amount of MAPK activation and receptor internalization were calculated as the average integrated intensities of the drug-treated wells divided by the average integrated intensities of the untreated wells and are expressed as percentages. Three to four replicates were performed for each time point or concentration for each independent experiment.

β-Arrestin Recruitment Assays. HEK293 cells were transiently transfected with β-$arrestin_2$-mRFP and either $HArCB_1$ pcDNA3 or $HArCB_2$ pcDNA3 and plated on to glass coverslips in 24-well dishes. Transient transfection of both receptor and β-$arrestin_2$ was used as we previously found that stable expression of either the receptor or β-$arrestin_2$ inhibited expression of the other, whether stably or transiently expressed. Cells were drug-treated for 7 min and fixed, and CB_1 or CB_2 receptors were detected as described above. Images of the fluorescently detected HA11 antibody and mRFP β-$arrestin_2$ were processed using MetaMorph software (Molecular Devices, Sunnyvale, CA). Line scans of pixel intensity were made across cells that expressed nonsaturating levels of β-$arrestin_2$-mRFP. Line scans of β-$arrestin_2$-mRFP and fluorescein isothiocyanate-anti-mouse (the presence of CB_2 receptor defines the cell membrane) were compared to determine the location of the outer cell membrane on the line scan. The average intensity of β-$arrestin_2$-mRFP was assessed at this point (within 1 μm of the membrane edge) and divided by the average intensity of mRFP in the cytosol to obtain a membrane/cytosol ratio. Membrane/cytosol ratios greater than 1 were interpreted as membrane recruitment of β-$arrestin_2$-mRFP.

Voltage-Gated Calcium Channel Recording. Calcium channel activity was measured by recording barium currents from wild-type untransfected AtT20 cells and AtT20 cells stably expressing rCB_1 or mCB_2 in the whole-cell configuration. The cells were voltage-

clamped at a holding potential of −70 mV. Voltage-activated currents were evoked by depolarizing the cells to 0 mV for 30 ms from the holding potential every 10 s. Currents were measured near the end of each 300-ms voltage step. Cd^{2+}-insensitive currents were subtracted offline, and the Cd^{2+}-sensitive current was taken to be the barium current flowing through calcium channels. In some experiments, we observed linear rundown of barium currents. In these cases, we used linear regression analysis to determine the rates of current rundown before drug application. Drug effects were determined by measuring the difference between the actual and predicted current on the basis of these rates of rundown.

Statistical Analysis. Data are reported as mean ± S.E.M. (except EC_{50}, IC_{50}, and $t_{1/2}$ data are reported as mean ± 95% confidence interval). Nonlinear regression was used to fit the concentration response curves and the time courses of receptor internalization. Student's *t* tests and one-way ANOVA with Bonferroni's multiple comparisons or Dunnett post tests were used where indicated. All graphs and statistical analyses were generated using Prism 4.0 software (GraphPad Software, San Diego, CA). Densitometric analysis was performed using ImageJ software (http://rsbweb.nih.gov/ij/).

Results

Ligand-Directed Internalization of rCB_1 and rCB_2 Receptors in HEK293 Cells. To measure cannabinoid receptor internalization, we employed HEK293 cells stably expressing HA-tagged rat CB_1 (rCB_1) and rat CB_2 (rCB_2) receptors. In these cells, internalization is inversely proportional to receptor level (i.e., the higher the surface levels of the receptor, the lower the maximal internalization). Thus, we used stable cell lines with similar surface expression levels (as assessed by quantitative on-cell Western analysis [Supplemental Fig. 1A; rCB_1, 1.0 ± 0.05; rCB_2, 1.1 ± 0.07 (relative units), $p = 0.11$]. However, the rCB_2 cells had a higher total expression level than rCB_1 cells (1.9-fold higher) as assessed by conventional Western blot analysis (Supplemental Fig. 1, B and C). This discrepancy between total protein level and surface level is probably due to the constitutive internalization of CB_2 observed by others, leading to a larger intracellular pool of CB_2 (Bouaboula et al., 1999). Nevertheless, because these two cell lines had nearly identical surface levels under basal conditions, this enabled us to compare internalization as a result drug treatments between these two cell lines.

CP55,940 and WIN55,212-2 are widely used and are generally regarded as nonselective, highly potent and efficacious CB_1 and CB_2 receptor agonists (Howlett et al., 2002). Figure 1A shows the time course of rCB_1 and rCB_2 internalization produced by 100 nM CP55,940. CP55,940 treatment internalizes both rCB_1 and rCB_2 to a similar extent, reaching a plateau of 56 ± 3.2% of basal surface levels in rCB_1-expressing cells and 59 ± 1.3% in rCB_2-expressing cells. rCB_2 internalized much more rapidly with a half-life of 8.2 min (5.6–15 min) compared with 36 min (24–71 min) for rCB_1. CP55,940 promoted internalization of rCB_1 and rCB_2 (Fig. 1B) with nearly equal potencies [rCB_1, EC_{50} = 0.48 nM (0.17–1.4 nM); rCB_2, EC_{50} = 1.3 nM (0.68–2.3 nM)] and efficacies [rCB_1, E_{max} = 56 ± 2.0% basal surface levels; rCB_2, E_{max} = 59 ± 1.2% of basal surface levels]. In rCB_1 cells, 100 nM CP55,940-induced internalization could be blocked by 1 μM rimonabant, a CB_1 receptor antagonist/inverse agonist (Fig. 1C; 93 ± 3.0% of basal surface levels, $p <$ 0.001 versus CP55,940 alone). For rCB_2 cells, 1 μM AM630, a CB_2 receptor antagonist, attenuated internalization by CP55,940 (Fig. 1C; 83 ± 1.8% of basal surface levels, $p < 0.001$ versus CP55,940 alone). As expected from previous work, WIN55,212-2 also produced rCB_1 receptor internalization (Fig. 1D) with a maximal internalization of 45 ± 3.4% of basal surface levels and a half-life of 34 (24–57) min. We were surprised to find that 100 nM WIN55,212-2 did not produce any rCB_2 internalization, even after 180 min of treatment (Fig. 1D). This was not a consequence of the concentration used as even 1 μM WIN55,212-2 did not produce rCB_2 internalization (Fig. 1E). Rimonabant (1 μM) could also prevent 1 μM WIN55,212-2 from internalizing rCB_1 (Fig. 1F; 96 ± 4.8% of basal surface levels, $p < 0.001$ versus WIN55,212-2 alone). AM630 had no effect on surface CB_2 during WIN55,212-2 treatment (Fig. 1F). Figure 1G provides representative images of cells treated with 100 nM CP55,940 or WIN55,212-2 for 120 min and also cotreatments with antagonists. It is of interest that the pattern of internalization differs between the two cell lines, with rCB_2 internalization resulting in more perinuclear localization of the receptor than for rCB_1, suggesting that internalized CB_1 and CB_2 may localize to different endosomal compartments. To test whether cannabinoid receptor internalization observed here was dependent on G protein activation, cells were treated overnight with 400 ng/ml PTX. PTX did not alter the magnitude (Supplemental Fig. 2A) of CP55,940 and WIN55,212-2 induced receptor internalization in either rCB_1 or rCB_2 cells. It also did not alter the kinetics of internalization for rCB_1 [CP55,940, 45 (27–145) min; WIN55,212-2, 54 (31–192) min] or rCB_2 [CP55,940, 11 (8.0–18) min]. This suggests that this internalization is independent of $G_{i/o}$ G protein activation. It is noteworthy that despite the inability to alter the kinetics or magnitude of agonist-induced receptor internalization, PTX did produce a small but significant increase in basal receptor surface levels in rCB_1 cells (110 ± 2.2% of basal surface levels, $p = 0.033$ versus untreated) and a larger increase in rCB_2 cells (130 ± 1.9% of basal surface levels, $p < 0.0001$ versus untreated), suggesting that $G_{i/o}$ G protein activation may play a role in basal cannabinoid receptor trafficking (Supplemental Fig. 2C). To determine whether or not the internalization we observed in these cells was clathrin-mediated, we treated these cells with CP55,940 and WIN55,212-2 in the presence of 350 mM sucrose, which blocks clathrin-mediated endocytosis (Hsieh et al., 1999). Sucrose completely prevented CP55,940-induced internalization of both rCB_1 and rCB_2 (Supplemental Fig. 2A; rCB_1, 96 ± 1.1% of basal surface levels, $p < 0.001$ versus CP55,940 alone; CB_2, 93 ± 2.8% of basal surface levels, $p < 0.001$ versus CP55,940 alone) and rCB_1 internalization as a result of WIN55,212-2 treatment (Supplemental Fig. 2B; 93 ± 3.8% of basal surface levels, $p <$ 0.001 versus WIN55,212-2 alone). Sucrose alone did not significantly alter rCB_1 surface levels but produced a small, yet statistically significant increase in rCB_2 surface levels (110 ± 0.77% of basal levels, $p = 0.010$) (Supplemental Fig. 2C).

There have been reports that rCB_2, mCB_2, and hCB_2 receptors possess significantly different pharmacological profiles despite each being a CB_2 receptor (Mukherjee et al., 2004; Bingham et al., 2007). Thus, the effect of WIN55,212-2 observed above may be unique to the rat CB_2 receptor. Furthermore, the cellular environment may also be a contributing factor. To test these possibilities, we treated HEK293 cells expressing mCB_2 or hCB_2 receptors as well as AtT20 cells expressing rCB_2 or mCB_2 receptors with CP55,940 or WIN55,212-2 (Supplemental Fig. 3A). In all cell lines, we obtained a pattern of results similar to that observed in our rCB_2 HEK293 cells. CP55,940 (100 nM) promoted CB_2 recep-

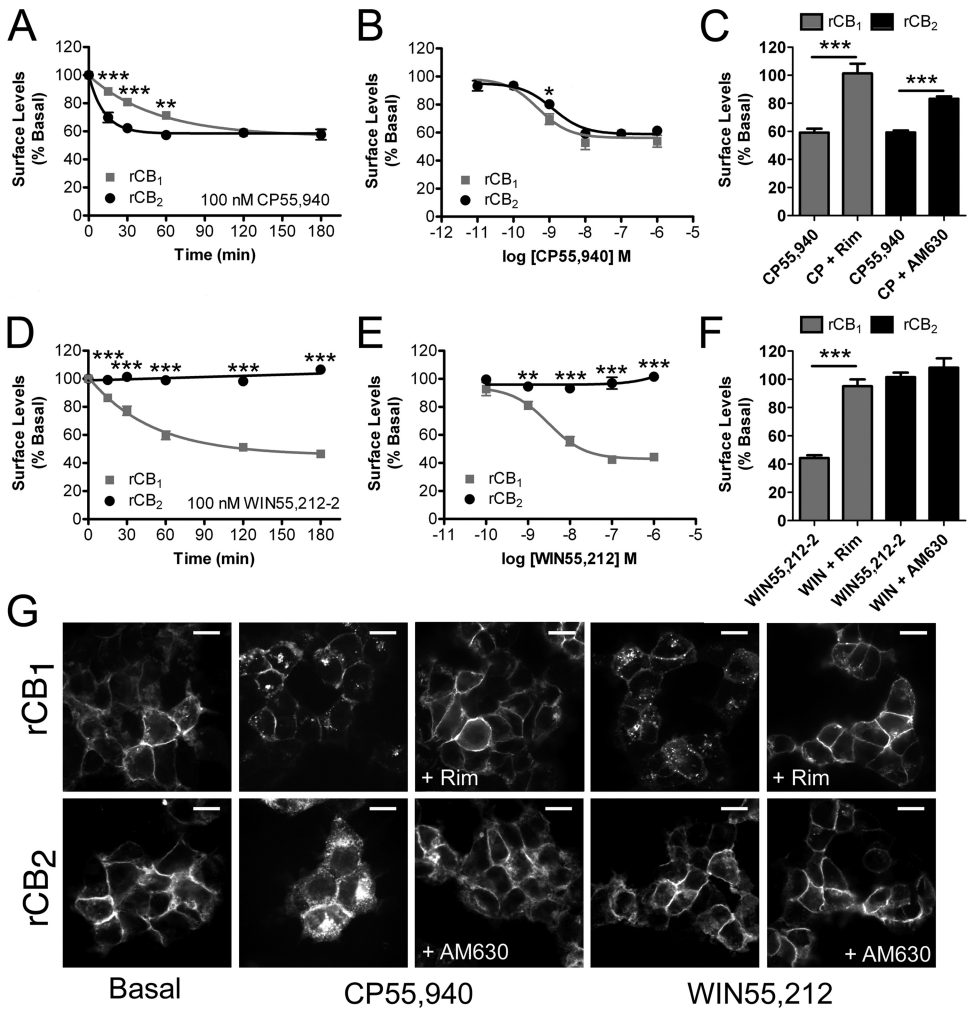

Fig. 1. CP55,940 and WIN55,212-2 differ in their abilities to internalize rCB_2 but not rCB_1 cannabinoid receptors. A, In rCB_1- and rCB_2-expressing HEK293 cells, 100 nM CP55,940 results in receptor internalization (n = 6–26 for each time point). B, 2 h of exposure to CP55,940 internalized rCB_1 and rCB_2 in a concentration-dependent manner (n = 3–26 for each concentration). C, 1 μM rimonabant (Rim) and 1 μM AM630 prevent receptor internalization by 100 nM CP55,940 treatment in rCB_1 (n = 3) and rCB_2 cells (n = 10), respectively. D, 100 nM WIN55,212-2 results in robust rCB_1 but not rCB_2 receptor internalization (n = 7–11). E, 2 h of exposure to WIN55,212-2 internalized rCB_1 in a concentration-dependent manner but not rCB_2 (n = 4–6). F, 1 μM rimonabant prevents receptor internalization by 100 nM WIN55,212-2 (WIN) treatment in rCB_1 (n = 5) but AM630 does not alter the effect of WIN55,212-2 on rCB_2 cells (n = 4). G, representative images of rCB_1 and rCB_2 cells treated with 100 nM CP55,940 or 100 nM WIN55,212-2 for 2 h. Cotreatment with 1 μM rimonabant and 1 μM AM630 is also shown. Scale bars, 20 μm. Data in A through F analyzed using unpaired Student's t tests. *, $p < 0.05$; **, $p < 0.01$; ***, $p < 0.001$.

tor internalization in each cell line, whereas 1 μM WIN55,212-2 produced little if any internalization. The effect of CP55,940 could be significantly inhibited by a cotreatment with 1 μM SR144528 in all cell lines and by 1 μM AM630 in the rCB_2 AtT20 cell lines and all the HEK293 cell lines. AM630 attenuated the effects of CP55,940 in the mCB_2 AtT20 cell line, but this difference did not reach statistical significance. This is probably due to the high expression level of mCB_2 in these cells, which may also account for the reduced effectiveness of CP55,940 in promoting receptor internalization in these cells. Nonetheless, the general pharmacological pattern is consistent across all cell lines.

It is also a possibility that the lack of internalization observed here for WIN55,212-2 was due to the presence of the HA-epitope tag found on the N terminus of the CB_2 receptors. To determine this, we measured receptor internalization induced by CP55,940 and WIN55,212-2 of untagged hCB_2 stably expressed in HEK293 cells. In these experiments, we used an antibody directed toward the N terminus of CB_2. We observed results similar to those with the HA-tagged receptors: CP55,940 promoted internalization of the untagged CB_2 receptor (74 ± 5.1% of basal surface levels), and WIN55,212-2 was ineffectual (100 ± 3.8% of basal surface levels) (Supplemental Fig. 3B). Taken together, these data suggest that the results we obtained in our internalization experiments are not limited to a specific cell type, species of CB_2 or the presence of an epitope tag.

Because we found such a profound difference between two ligands that are widely considered to be interchangeable CB_2 agonists, we expanded our study to include a range of cannabinoid receptor ligands. Figure 2 provides the concentration response curves after 2 h of treatment with each of these ligands, grouped by ligand family. Supplemental Table 1 provides a summary of the data displayed in Fig. 2, giving EC_{50} values and maximal internalization achieved. For all ligands that produced internalization, we also determined efficacy of antagonist block using 1 μM rimonabant for rCB_1 and 1 μM AM630 for rCB_2 cells. For all ligands, we found that rimonabant could significantly block internalization in rCB_1 cells and AM630 in rCB_2 cells (Supplemental Fig. 4). Figure 2, A_1 and A_2, details the effects of aminoalkylindoles, the same class of ligand to which WIN55,212-2 belongs. It is noteworthy that all aminoalkylindoles tested produced modest to no internalization of rCB_2 receptors (Fig. A2) and (2-iodo-5-nitrophenyl)-[1-[(1-methylpiperidin-2-yl)methyl]indol-3-yl]methanone (AM1241), reported to be a CB_2-selective agonist, slightly increased surface levels of rCB_2. (2-Methyl-1-propyl-1*H*-indol-3-yl)-1-naphthalenylmethanone (JWH015), frequently used as a "CB_2-selective agonist," significantly internalized rCB_1 (Fig. $2A_1$). This was markedly greater than the internalization produced in rCB_2 cells (p = 0.0015). THC did not produce any rCB_2 internalization, but (6*aR*,10*aR*)-3-(1,1-dimethylbutyl)-6*a*,7,10,10*a*-tetrahydro-6,6,9-trimethyl-6*H*-dibenzo[*b*,*d*]pyran (JWH133), THCV, and HU210 did, despite being structurally similar to THC (Fig.

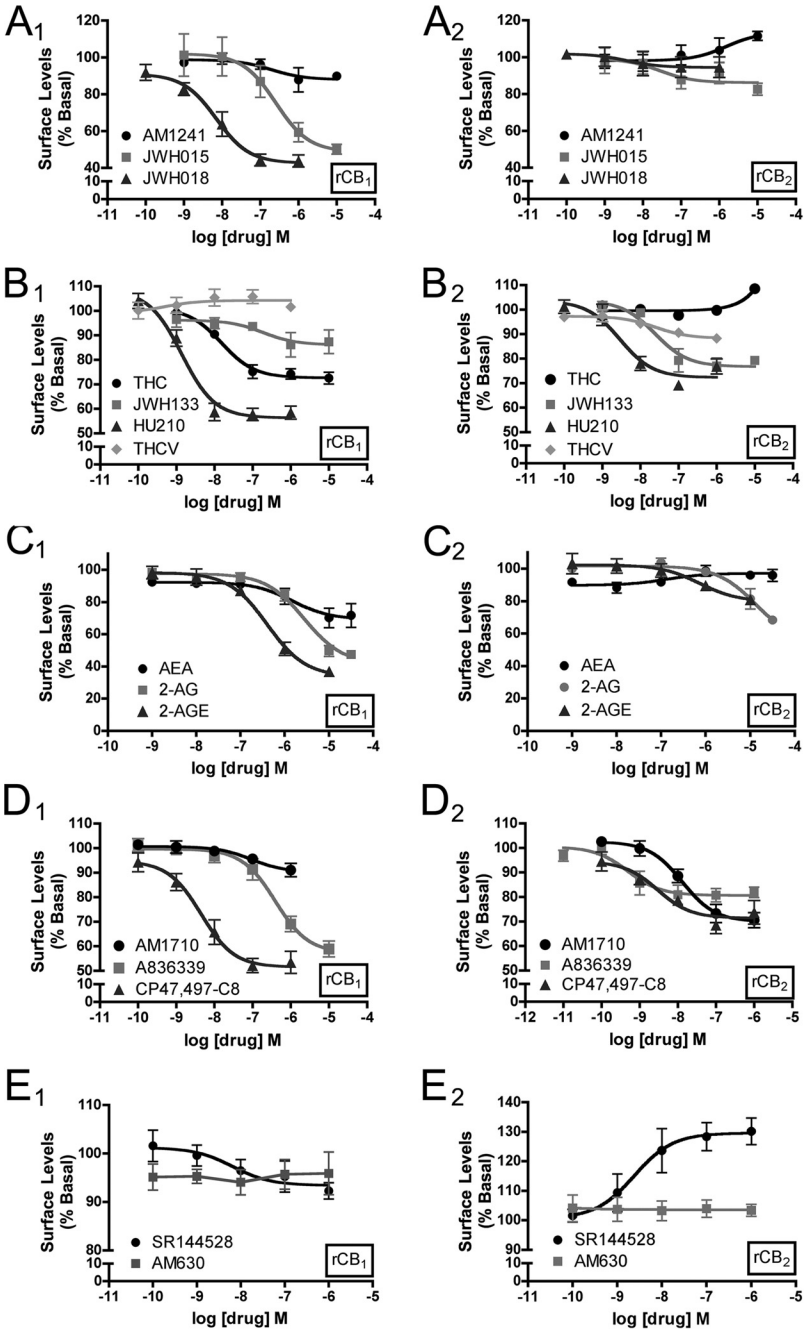

Fig. 2. Concentration response curves for internalization by various agonists and ligands in rCB_1- and rCB_2-expressing HEK293 cells. Concentration response curves for rCB_1-expressing (A_1–E_1, left) and rCB_2-expressing (A_2–E_2, right) HEK293 cells after 2 h of treatments with aminoalkylindoles (n = 3–5) (A_1 and A_2), classic cannabinoids (n = 3–6) (B_1 and B_2), and endocannabinoids (n = 3–5) (C_1 and C_2). D_1 and D_2, the iminothiazole A-836339 (n = 3–5) and the cannabilactone AM1710 (n = 4). CP47,497-C8 data from Atwood et al. (2011) included for comparison. E_1 and E_2, concentration response curves for rCB_1 and rCB_2 cells treated with the CB_2 antagonists SR14428 and AM630 (n = 4–5). 2-AGE, 2-arachidonoylglyceryl ether.

$2B_2$). The iminothiazole compound *N*-[3-(2-methoxyethyl)-4,5-dimethyl-1,3-thiazol-2-ylidene]-2,2,3,3-tetramethylcyclopropane-1-carboxamide (A-836339) potently produced moderate rCB_2 internalization as did the cannabilactone AM1710 (Fig. $2D_2$) (Rahn et al., 2011). A-836339 also produced extensive rCB_1 internalization, but its EC_{50} for rCB_1 internalization was approximately 800-fold higher than that for rCB_2 (Fig. $2D_1$). AM1710 and JWH133 were the only compounds that produced greater internalization of rCB_2 than rCB_1. We also confirmed that SR144528 increased surface levels of CB_2 (Bouaboula et al., 1999); interestingly, however, AM630, a structurally distinct CB_2 receptor antagonist, did not significantly increase cell surface CB_2 (Fig. $2E_2$). Rimonabant had no effect on either rCB_1 or rCB_2 surface levels (Supplemental Table 1).

As shown in Fig. $2C_1$, the endocannabinoids 2-AG and AEA produced some internalization in rCB_1 cells, albeit at very high concentrations. This may be due to the low intrinsic activity of these ligands for internalization or to endocannabinoid breakdown via catabolic enzymes endogenously expressed in HEK293 cells. Fatty acid amide hydrolase (FAAH) is the enzyme primarily responsible for breakdown of anandamide (Cravatt et al., 2001; Ligresti et al., 2005), whereas monoacylglycerol lipase (MGL) is reported to be the enzyme that is primarily responsible for the degradation of 2-AG, although other enzymes contribute (Blankman et al., 2007). HEK293 cells possess significant levels of mRNA (as assessed by microarray analysis) for enzymes involved in endocannabinoid synthesis and degradation including FAAH (Supplemental Fig. 5A). We detected MGL mRNA, but at a statistically insignificant level, although other enzymes that

may degrade 2-AG were detected at significant levels (α/β-hydrolases 6 and 12). URB597, a selective inhibitor of FAAH, effectively increased the ability of low concentrations of AEA to promote rCB_1 internalization (Supplemental Fig. 5B) but had little effect on rCB_2 internalization (Supplemental Fig. 5C). URB597 (100 nM) treatment shifted the EC_{50} of AEA-mediated rCB_1 internalization from 1.5 μM (0.1–16 μM) to 64 nM (13–320 nM). Maximal internalization was not significantly increased (30 μM AEA: 69 ± 4.7% basal surface levels; 30 μM AEA + 100 nM URB597: 56 ± 3.4% of basal surface levels). JZL184, an inhibitor of MGL (Long et al., 2009), did not produce a shift in the concentration response curves for either rCB_1 or rCB_2 (Supplemental Fig. 5, B and C).

WIN55,212-2 Competitively Antagonizes Agonist-Induced rCB_2 Receptor Internalization. Because CP55,940 produced robust rCB_2 internalization and WIN55,212-2 produced no internalization, it is possible that WIN55,212-2 could competitively antagonize CP55,940 internalization. Figure 3A shows a time course of rCB_2 internalization produced by treatment with 100 nM CP55,940 alone or with increasing concentrations of WIN55,212-2 as a cotreatment. WIN55,212-2 prevents CP55,940-induced rCB_2 internalization, and this was concentration-dependent. The same was not true for rCB_1 cells in which WIN55,212-2 (100 nM or 1 μM) had no effect on the internalization induced by 100 nM CP55,940 (Fig. 3B). Figure 3C shows representative images of rCB_1 or rCB_2 cells cotreated with 100 nM CP55,940 and 1 μM WIN55,212-2. To further explore the concentration dependence of this effect, we performed two complementary experiments with rCB_1 and rCB_2 cells. First, we applied a constant 100 nM CP55,940 with cotreatments of increasing concentrations of WIN55,212-2. WIN55,212-2 concentration-dependently reduced CP55,940-induced internalization in rCB_2 cells, but not in rCB_1 cells (Fig. 3D). We then repeated the experiment, but this time with a constant 100 nM WIN55,212-2 and increasing concentrations of CP55,940 (Fig. 3D). Increasing concentrations of CP55,940 overcame the antagonistic effect of WIN55,212-2 on rCB_2 internalization but had no effect on rCB_1 internalization. To further explore the mechanistic basis of the antagonistic effect of WIN55,212-2, we performed the same experiment as above: a fixed concentration of WIN55,212-2 with increasing concentrations of CP55,940 over a wide range of concentrations of WIN55,212-2 as a cotreatment. As seen in Fig. 3E, increasing concentrations of WIN55,212-2 shifted the CP55,940 concentration curve to the right as would a rCB_2 antagonist. We constructed a Schild plot of these data (Fig. 3F) to determine whether the antagonistic effect of WIN55,212-2 was competitive in nature. The slope of the line obtained in the Schild plot analysis was 0.98 ± 0.065, suggesting that WIN55,212-2 competitively antagonizes CP55,940-induced rCB_2 internalization. WIN55,212-2 was also able to block CP55,940-induced CB_2 internalization in both HEK293 and AtT20 cells and in cells expressing mCB_2 and hCB_2 (Supplemental Fig. 3A). This once again suggests that the effects of WIN55,212-2 are not unique to rCB_2 or HEK293 cells. WIN55,212-2 was also not unique in its ability to prevent CP55,940-induced rCB_2 internalization. Figure 3G shows data obtained using 10 nM CP55,940 and cotreatments with 100 nM and 1 μM concentrations of other ligands. Other ligands from the same aminoalkylindole class as WIN55,212-2 (AM1241 and JWH015) also antagonized CP55,940-induced internalization. AM1241 was more potent of an antagonist than JWH015. THC, a low-efficacy CB_2 agonist in most assays, also antagonized CP55,940-induced rCB_2 internalization. Other classic cannabinoids, THCV and JWH133, had little to no effect on the ability of CP55,940 to promote rCB_2 internalization. The CB_2 antagonists AM630 and SR144528 blocked internalization as expected. The endocannabinoid 2-AG had no effect. A-836339 also could antagonize the internalization obtained using CP55,940, consistent with its high affinity for CB_2, but low efficacy to promote internalization (Fig. 2, D_1 and D_2). AM1710 had no effect. Thus it seems that WIN55,212-2, other aminoalkylindoles, and some low internalizing CB_2 ligands, such as THC and A-836339, all can antagonize CP55,940-induced rCB_2 internalization.

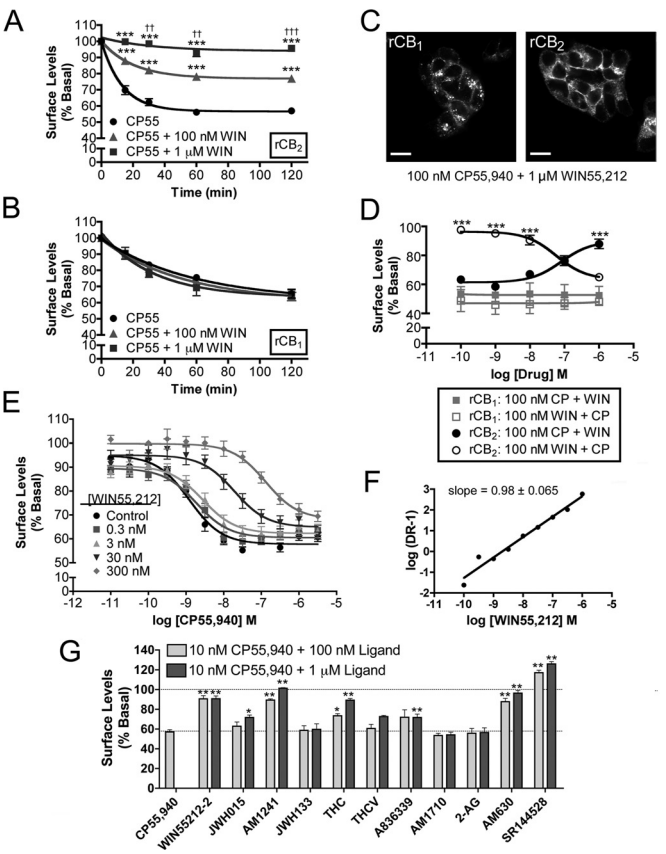

Fig. 3. WIN55,212-2 and other aminoalkylindoles antagonize CP55,940-induced rCB_2 internalization. A, time course of 100 nM CP55,940 (CP55)-induced internalization of rCB_2 in HEK293 cells. Cotreatment with 100 nM CP55,940 and 1 μM WIN55,212-2 (WIN) attenuates CP55,940-mediated internalization. ***, $p < 0.001$ versus CP55,940 alone. ††, $p < 0.01$; †††, $p < 0.001$, 100 nM WIN55,212-2 versus 1 μM WIN55,212-2 (n = 4–6). B, WIN55,212-2 has no effect on CP55,940-mediated rCB_1 internalization (n = 3–12). C, representative images of rCB_1 and rCB_2 HEK293 cells treated with the combination of 100 nM CP55,940 and 1 μM WIN55,212-2. Scale bars, 20 μm. D, rCB_1 or rCB_2 cells were cotreated with 100 nM CP55,940 (CP) and increasing concentrations of WIN55,212-2 (closed symbols) or alternatively cotreated with 100 nM WIN55,212-2 and increasing concentrations of CP55,940 (open symbols). ***, $p < 0.001$, CP + WIN versus WIN + CP (n = 3–15). E, individual concentration curves of CP55,940 with indicated concentrations of WIN55,212-2 cotreatments (n = 6–27). F, Schild plot constructed from data in E. The slope indicates that the interaction between CP55,940 and WIN55,212-2 is competitive. G, cotreatments of rCB_2 HEK293 cells with 10 nM CP55,940 and 100 nM or 1 μM concentrations of the indicated ligands (n = 3–17). *, $p < 0.05$; **, $p < 0.01$, versus CP55,940 alone. Data in A, B, and G analyzed using one-way ANOVA with Bonferroni's multiple comparison test. Data in D analyzed using Student's t test.

WIN55,212-2 Engages rCB_2 to Activate Specific Signaling Pathways: Evidence for Functional Selectivity. After these experiments demonstrating that WIN55,212-2 not only failed to promote rCB_2 internalization but actually antagonized it, we were concerned whether WIN55,212-2 was capable of activating rCB_2 in our cell lines. To test this possibility, we performed two different types of experiments. First we tested whether CP55,940 and WIN55,212-2 could activate ERK1/2 (p42/44) MAPK. Second, we analyzed the ability of these two compounds to promote β-arrestin$_2$ recruitment in cells coexpressing rCB_2 (or rCB_1 as a control) and β-arrestin$_2$.

We used the same cell lines that were used for the internalization assays to measure levels of phospho-ERK1/2. In rCB_1 HEK293 cells, ERK1/2 activation was maximal after 5 min of treatment (Fig. 4A) for both 100 nM CP55,940 (220 ± 8.7% of basal levels) and 100 nM WIN55,212-2 (200 ± 7.6% of basal levels). There was a significant difference in the amount of MAPK activation achieved by each drug treatment only at 5 min ($p = 0.043$). We repeated this time course experiment with rCB_2 HEK293 cells and found that both 100 nM CP55,940 and WIN55,212-2 could activate MAPK (Fig. 4B). It is noteworthy that CP55,940 reached maximal activation at 5 min of treatment (160 ± 2.4% of basal levels) similar to the timing of the peak in rCB_1 cells, but WIN55,212-2 produced a somewhat more prolonged activation than CP55,940, reaching a peak between 5 and 7.5 min (5 min, 140 ± 3.5% of basal levels; 7.5 min, 140 ± 3.4% of basal levels, ns). CP55,940 and WIN55,212-2 activated ERK1/2 in rCB_1 HEK293 cells in a concentration-dependent manner with CP55,940 being significantly more potent [EC_{50} = 1.4 nM (0.56–3.3 nM)] than WIN55,212-2 [EC_{50} = 19 nM (9.0–40 nM)] (Fig. 4C). We found no differences in maximal efficacies [CP55,940, E_{max} = 220 ± 5.2% of basal levels; WIN55,212-2, E_{max} = 220 ± 6.9% of basal levels]. In rCB_2 cells, treatments with both compounds resulted in MAPK activation that was also concentration-dependent (Fig. 4D). CP55,940 was somewhat more potent than WIN55,212-2 [CP55,940, EC_{50} = 0.56 nM (0.18–22 nM); WIN55,212-2, EC_{50} = 2.6 nM (0.49–13 nM)]. CP55,940 was significantly more efficacious (CP55,940, E_{max} = 150 ± 2.3% of basal levels) than WIN55,212-2 (E_{max} = 140.0 ± 2.5% of basal levels). In rCB_1 cells, 1 μM rimonabant inhibited the effects of 100 nM CP55,940 (Fig. 4C; 102 ± 7.0% of basal levels, $p < 0.0001$ versus CP55,940 alone) and 100 nM WIN55,212-2 (94 ± 6.4% of basal levels, $p < 0.0001$ versus WIN55,212-2 alone), and 1 μM AM630 did the same in rCB_2 cells (Fig. 4D; 120 ± 6.0% of basal levels, $p < 0.0001$ versus CP55,940; 99 ± 1.0% of basal levels, $p < 0.0001$ versus WIN55,212-2). Receptor-independent activation of ERK1/2 MAPK using phorbol 12-myristate 13-acetate resulted in much higher levels of MAPK activation (rCB_1, 420 ± 84% of basal; rCB_2, 400 ± 29%; native HEK293 cells, 380 ± 22%) demonstrating that the maximal effects by WIN55,212-2 and CP55,940 were nonsaturating (Supplemental Fig. 6). CP55,940 and WIN55,212-2 had no effect on ERK1/2 phosphorylation in untransfected HEK293 cells (CP55,940, 100 ± 2.2% basal; WIN55,212-2, 100 ± 3.7% basal).

We next looked at β-arrestin membrane recruitment as an indicator of receptor activation. β-arrestins are proteins that are recruited to activated GPCRs and prevent the association of the activated receptor with its G proteins and later may serve as scaffolds to recruit signaling complexes to the GPCR (Rajagopal et al., 2010). β-Arrestin recruitment can be observed as a redistribution of fluorescently labeled β-arrestin from the cytosol to the membrane after drug treatment and has been characterized in rCB_1-expressing HEK293 cells (Daigle et al., 2008). To determine whether β-arrestin translocated in this manner in response to CP55,940 and WIN55,212-2, we transiently transfected HEK293 cells with either rCB_1 or rCB_2 and β-arrestin$_2$ with a mRFP tag. Figure 5A shows HEK293 cells that express rCB_1 (bottom) and β-arrestin$_2$-mRFP (top) after various treatments. After treatment with either 100 nM CP55,940 or 100 nM WIN55,212-2, β-arrestin$_2$-mRFP moved from a predominantly cytosolic distribution (Fig. 5A, 1) to a more membrane-associated distribution (Figs. 5A, 2 and 4, respectively). This effect could be prevented by 1 μM rimonabant (Figs. 5A, 3 and 5). Figure 5C quantifies the data obtained with these rCB_1-expressing cells. The basal membrane/cytosol ratio was 0.91 ± 0.038. CP55,940 (100 nM) significantly promoted β-arrestin$_2$ membrane recruitment, increasing the membrane/cytosol ratio to 1.3 ± 0.060 ($p < 0.001$ versus untreated) as did 100 nM WIN55,212-2 (1.4 ± 0.10, $p < 0.001$ versus untreated). Rimonabant prevented this recruitment for both CP55,940 (0.83 ± 0.050, $p < 0.001$ versus CP55,940) and WIN55,212-2

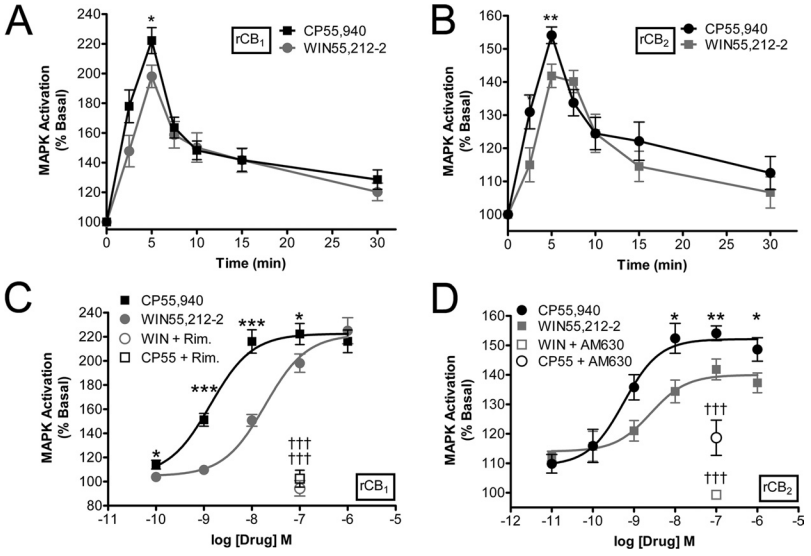

Fig. 4. CP55,940 and WIN55,212-2 promote MAPK activation in rCB_1- and rCB_2-expressing HEK293 cells. A, Time course of MAPK activation in rCB_1 HEK293 cells with 100 nM CP55,940 and 100 nM WIN55,212-2 (n = 9–21). *, $p < 0.05$ CP55,940 versus WIN55,212-2. B, same as in A, but with rCB_2 HEK293 cells (n = 7–22). **, $p < 0.01$ CP55,940 versus WIN55,212-2. C, concentration-response curves for 5 min treatments with increasing concentrations of CP55,940 (CP55) and WIN55,212-2 (WIN) in rCB_1 HEK293 cells. 1 μM rimonabant (Rim) blocks MAPK activation by 100 nM concentration of either agonist (n = 4–21). *, $p < 0.05$; ***, $p < 0.001$, CP55,940 versus WIN55,212-2. †††, $p < 0.001$, CP55,940 or WIN55,212-2 versus antagonist. D, concentration-response curves for 5-min treatments with increasing concentrations of CP55,940 or WIN55,212-2 in rCB_2 HEK293 cells (n = 5–22). 1 μM AM630 blocks MAPK activation by 100 nM concentration of either agonist. Data analyzed using unpaired Student's t test. *, $p < 0.05$; ** $p < 0.01$, CP55,940 versus WIN55,212-2. †††, $p < 0.001$, CP55,940 or WIN55,212-2 versus antagonist.

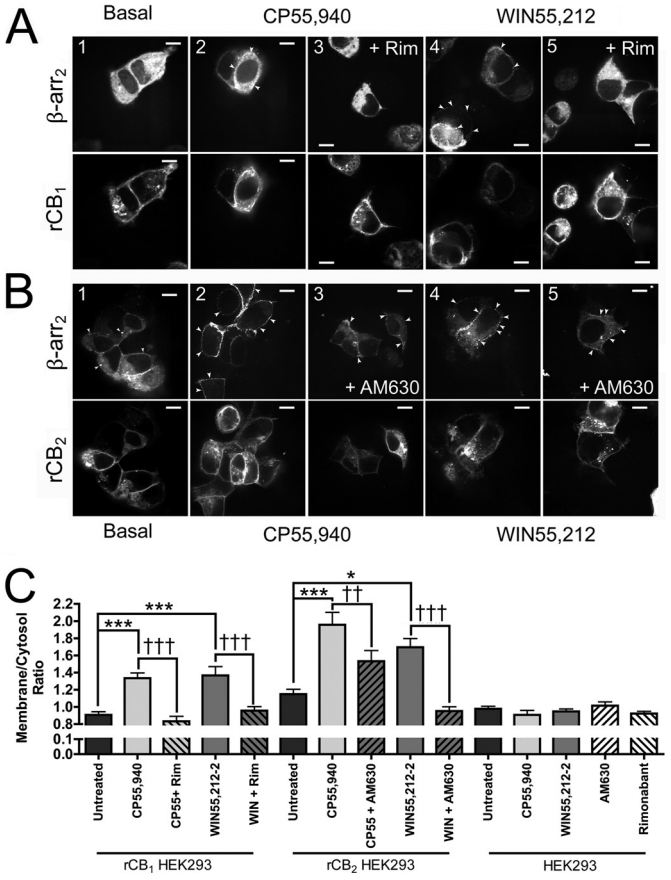

Fig. 5. CP55,940 and WIN55,212-2 promote recruitment of β-arrestin$_2$ to the membrane in rCB$_1$- and rCB$_2$-expressing HEK293 cells. A, HEK293 cells transiently expressing rCB$_1$ and β-arrestin$_2$-mRFP were treated with 100 nM CP55,940 or 100 nM WIN55,212-2 with or without 1 μM rimonabant. Top, β-arrestin$_2$-mRFP (βarr$_2$). Bottom, staining for rCB$_1$ (anti-HA primary antibody). Arrowheads indicate examples of membrane recruitment of β-arrestin$_2$. Scale bars, 10 μm. B, same as in A but with rCB$_2$ transiently expressed instead of rCB$_1$. 100 nM CP55,940, 1 μM WIN55,212-2, and 1 μM AM630 were used in the treatments. C, quantification of data from rCB$_1$ cells (n = 6–14), rCB$_2$ cells (n = 10–13), and native HEK293 cells (n = 5). Increases in membrane/cytosol ratio indicate β-arrestin$_2$ membrane recruitment. Data in C analyzed using one-way ANOVA with Bonferroni's multiple comparison test. *, $p < 0.05$; ***, $p < 0.001$, versus untreated. ††, $p < 0.01$; †††, $p < 0.001$, CP55,940 or WIN55,212-2 versus antagonist.

(0.96 ± 0.050, $p < 0.001$ versus WIN55,212-2). Repeating this experiment, but this time with HEK293 cells transiently expressing rCB$_2$ instead of rCB$_1$, we obtained similar results. It is noteworthy that even in untreated rCB$_2$ cells, a substantial fraction of β-arrestin$_2$ was already at the membrane (Fig. 6, B1 and C; membrane/cytosol ratio, 1.15 ± 0.060). This is probably due to constitutive activity of CB$_2$ as noted by others in CB$_2$-overexpressing cells (Bouaboula et al., 1999). However, despite the basal membrane localization, 100 nM CP55,940 significantly increased membrane recruitment (Fig. 5, B2 and C; 2.1 ± 0.15 $p < 0.001$ versus untreated). AM630 attenuated this effect (Fig. 5, B3 and C; 1.5 ± 0.12 $p < 0.01$ versus CP55,940, ns versus untreated). WIN55,212-2 (1 μM) promoted significant translocation of β-arrestin$_2$ from the cytosol to the membrane in rCB$_2$ cells (Fig. 5, B4 and C; 1.6 ± 0.090, $p < 0.05$ versus untreated), and this was significantly inhibited by 1 μM AM630 (Fig. 6, B5 and C; 0.95 ± 0.050, $p < 0.001$ versus WIN55,212-2, ns versus untreated). Thus, although less potent than CP55,940, WIN55,212-2 is capable of activating rCB$_2$ to promote β-arrestin$_2$ membrane recruitment. Control experiments with HEK293 cells expressing only β-arrestin$_2$ did not reveal any effect of 1 μM WIN55,212-2, 100 nM CP55,940, 1 μM AM630, or 1 μM rimonabant on membrane localization of β-arrestin$_2$ (Fig. 5C; p = 0.28). This suggests that the effects seen with these drugs are indeed due to cannabinoid receptor activation and not to activation of other GPCRs that might be present in HEK293 cells. These two sets of results (β-arrestin and MAPK) convinced us that WIN55,212-2 is capable of activating rCB$_2$ and suggested that WIN55,212-2 may display functional selectivity with respect to internalization.

CB$_2$-Mediated Inhibition of Voltage Gated Calcium Channels: Further Evidence That WIN55,212-2 Is a Functionally Selective CB$_2$ Ligand. Early studies reported that CB$_2$ does not effectively modulate voltage gated calcium or G protein-regulated potassium channels (Felder et al., 1995; Ross et al., 2001). However, these studies employed WIN55,212-2 as the CB$_2$ agonist. On the basis of our internalization data, we hypothesized that WIN55,212-2 is a poor agonist at CB$_2$ with regard to inhibition of voltage-gated calcium channels (VGCCs). We revisited the calcium channel experiments done in AtT20 cells (Felder et al., 1995), comparing the effectiveness of WIN55,212-2 and CP55,940. For these experiments, we employed the mCB$_2$-expressing AtT20 cells used in Supplemental Fig. 3A. We also used wild-type, untransfected AtT20 cells and rCB$_1$-expressing AtT20 cells as controls. Figure 6, A and D, shows that 100 nM and 1 μM WIN55,212-2 failed to inhibit VGCCs in mCB$_2$-expressing AtT20 cells (0.4 ± 1.6 and −3.4 ± 3.2% inhibition, respectively). In contrast, 100 nM WIN55,212-2 inhibited VGCCs in rCB$_1$-expressing AtT20 cells (13 ± 3.8% inhibition) (Fig. 6E). CP55,940 (100 nM), as seen in Fig. 6, B and D, reduced the magnitude of barium currents in mCB$_2$-expressing cells in a concentration-dependent fashion [IC$_{50}$ = 18 nM (1.1–290.0 nM), E_{max} = 18 ± 2.2% inhibition]. Inhibition by 100 nM CP55,940 was blocked by 1 μM AM630 treatment (4.4 ± 2.7% activation) and was absent in untransfected wild-type cells (0.10 ± 3.1% inhibition) (Fig. 6E). It is noteworthy that on its own, 1 μM AM630 treatment significantly increased the magnitude of barium currents relative to control (Fig. 6, C and E; 12 ± 2.4% activation, not significantly different from CP55,940 + AM630); thus, AM630 acts as an inverse agonist. CP55,940 (100 nM) also inhibited VGCCs in rCB$_1$-expressing cells (13 ± 3.8% inhibition) (Fig. 6E). The effects of CP55,940 in rCB$_1$- and mCB$_2$-expressing cells was not statistically different. Supporting the inverse agonist effect of AM630, we found that oxotremorine-m, a muscarinic receptor agonist, was much more effective at inhibiting VGCCs in WT (16 ± 4.3% inhibition) than in mCB$_2$-expressing AtT20 cells (6.5 ± 1.8%, p = 0.025 versus rCB$_1$, p = 0.055 versus WT) (Fig. 6E), suggesting a constitutive inhibition of VGCC by CB$_2$, similar to the data presented by Felder et al. (1995). We also tested whether WIN55,212-2 could block the effects of CP55,940 as it did in our internalization studies. When 100 nM CP55,940 was applied in the presence of 1 μM WIN55,212-2, CP55,940 did not produce substantial inhibition (3.4 ± 4.3% inhibition, p = 0.29 versus WIN55,212-2 alone). These data demonstrate another instance in which WIN55,212-2 acted as a functional antagonist of CP55,940 at CB$_2$.

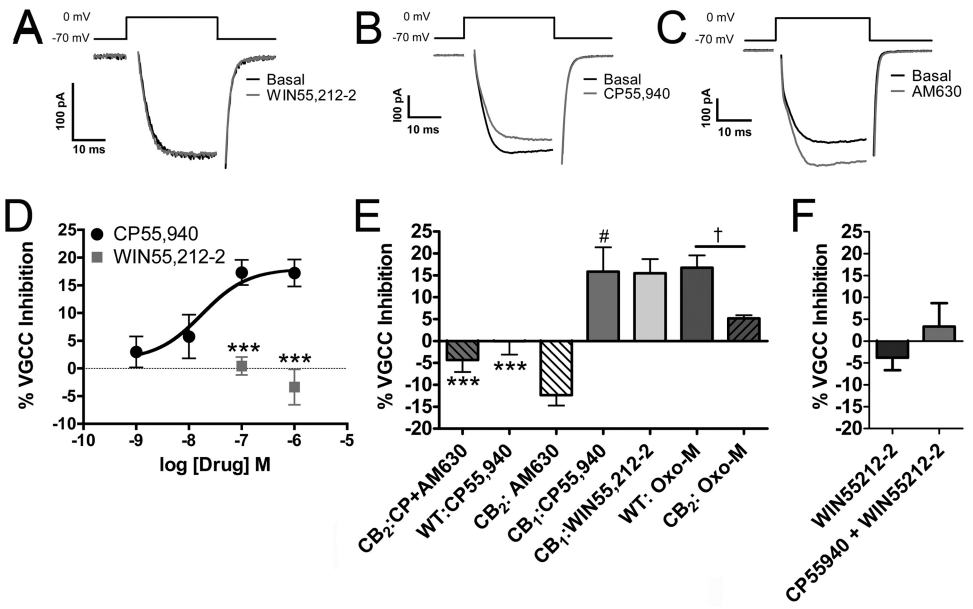

Fig. 6. CP55,940, but not WIN55,212-2, activates mCB_2 to inhibit voltage-gated calcium channels. Barium currents in AtT20 cells were elicited by depolarizing the cells to 0 mV for 30 ms from a holding potential of −70 mV. In mCB_2-expressing AtT20 cells, 100 nM WIN55,212-2 (A) had no effect on the amplitude of recorded currents, whereas 100 nM CP55,940 (B) inhibited calcium channels. C, 1 μM AM630 increased the magnitude of barium currents. D, CP55,940 inhibited voltage-gated calcium channels in a concentration-dependent manner ($n = 4$–17), whereas 100 nM ($n = 6$) and 1 μM WIN55,212-2 did not ($n = 7$). ***, $p < 0.001$, versus CP55,940. E, 1 μM AM630 blocked the effects of 100 nM CP55,940 in mCB_2-expressing AtT20 cells ($n = 4$) and increased the magnitude of barium currents on its own (as seen by a negative inhibition) ($n = 15$). 100 nM CP55,940 had no effect on calcium channels in wild-type (WT) untransfected cells ($n = 5$) but was able to inhibit calcium channels in rCB_1-expressing AtT20 cells ($n = 6$). 100 nM WIN55,212-2 inhibited voltage-gated calcium channels in rCB_1-expressing AtT20 cells ($n = 6$). 10 μM oxotremorine-M (oxo-M) inhibited calcium channels in untransfected HEK cells ($n = 9$). This inhibition was decreased in AtT20 cells stably expressing mCB_2 ($n = 9$). ***, $p < 0.001$, versus CP55,940 treatment of mCB_2 AtT20 cells. #, $p < 0.05$, versus WIN55,212-2 treatment of mCB_2 AtT20 cells. †, $p < 0.05$, versus Oxo-M treatment of mCB_2 AtT20 cells. F, 1 μM WIN55,212-2 does not affect the inhibition of VGCCs by 100 nM CP55,940. Data in D and F were analyzed using unpaired Student's t test. Data in E were analyzed using one-way ANOVA with Bonferroni's multiple comparison test.

Other Cannabinoid Ligands Display Functional Selectivity at CB_2. On the basis of the differences we observed between CP55,940 and WIN55,212-2, we sought to determine whether other cannabinoid ligands also demonstrated functional selectivity. Table 1 compares the efficacies of a select group of cannabinoid ligands in their abilities to activate ERK1/2 MAPK, promote β-$arrestin_2$-mRFP membrane recruitment, and inhibit VGCCs. Also included in Table 1 are data from Figs. 1 and 2 to allow comparisons of the abilities of these CB_2 ligands to promote internalization with their abilities to act on these other signaling pathways.

Because of the variable nature of the MAPK and β-arrestin recruitment experiments, we again tested CP55,940 and WIN55,212-2 for side-by-side comparisons with the other ligands. For MAPK experiments, we compared the levels of phospho-ERK1/2 activation obtained after 5 min of treatment with each ligand (Table 1). The effects of the ligands on MAPK in rCB_2-expressing HEK293 cells were compared with those on native HEK293 cells. We found that 2-AG, CP55,940, and WIN55,212-2 were the most efficacious CB_2 ligands in activation of ERK1/2. In contrast, AM1241, AM630, and SR144528 did not significantly affect phospho-ERK1/2 levels in rCB_2 HEK293 cells. We next tested the ability of these same ligands to promote β-$arrestin_2$ membrane recruitment in CB_2-expressing cells (Table 1). It is noteworthy that in this set of experiments, we did not see the basal level of β-$arrestin_2$ membrane recruitment that we previously saw (0.95 ± 0.024 membrane/cytosol ratio). However, we still observed robust membrane recruitment in response to CP55,940. We also saw recruitment after treatment with JWH133, AM1710, and A-836339. Each produced significantly more membrane recruitment of β-$arrestin_2$-mRFP than observed in untreated cells. No other ligand treatment induced significant levels of β-$arrestin_2$ membrane recruitment, although the effect of WIN55,212-2 was significantly blocked by AM630 ($p = 0.020$). Finally, we tested whether these ligands would inhibit VGCCs in the mCB_2-expressing AtT20 cells used in Supplemental Fig. 3A with native AtT20 cells used as controls (Table 1). We found that 2-AG was more efficacious than CP55,940 in inhibiting VGCCs. 2-AG did inhibit VGCCs in untransfected AtT20 cells (5.9 ± 1.4% inhibition); however, this effect was significantly less than in transfected AtT20 cells ($p = 0.016$). JWH133 and A-836339 also produced inhibition that was significantly greater than that of control. It is noteworthy that, like AM630 (Fig. 6, C and E), several other ligands acted as inverse agonists, increasing, rather than decreasing, VGCC activity. JWH015 had a minor inverse agonist effect on VGCC activity that was significantly different from that of control ($p = 0.023$) because of its inhibitory effect in nontransfected AtT20 cells (4.6 ± 0.60% inhibition). THCV produced the largest increase, although it was not statistically different from control ($p = 0.17$). THCV was followed by the CB_2 antagonists/inverse agonists AM630 and SR144528. Inverse agonism implies that CB_2 here is constitutively inhibiting VGCCs, because of ongoing synthesis of endogenous ligand or because a substantial fraction of the CB_2 receptors is active. Because of a recent report that demonstrated that 1-(2,3-dichloroben-

TABLE 1

Evidence for functionally selective CB_2 ligands

Cannabinoid ligands from multiple classes were tested for their abilities to activate ERK1/2 MAPK in rCB_2-expressing HEK293 cells, promote β-$arrestin_2$ membrane recruitment in HEK293 cells transiently transfected with rCB_2 and β-$arrestin_2$-mRFP, and inhibit VGCCs in mCB_2-expressing AtT20 cells. Positive values reflect inhibition of VGCCs and negative values reflect activation (e.g., inverse agonism). Protocols for each experiment were identical to those done in Figs. 4 to 6. Data for ERK1/2 and VGCC experiments were analyzed using unpaired Student's *t* test vs. native HEK293 or native AtT20 cells, respectively. Data for β-arrestin were analyzed using one-way ANOVA with Dunnett post-tests. Data for internalization from Figs. 1 and 2 and binding data obtained from the cited references are included for additional comparison. Drug concentrations: 10 μM 2-AG was used for internalization ($n = 12$), and 5 μM 2-AG was used for MAPK activation ($n = 6$–15), β-arrestin recruitment ($n = 5$–15), and VGCC inhibition ($n = 4$–17). All other drugs, 1 μM. Values without symbols are not statistically significant.

Drug	Internalization	MAPK Activation	β-Arrestin Recruitment	VGCC Inhibition	CB_2 K_i
	% basal		*membrane/cytosol ratio*	*% inhibition*	*nM*
CP55,940	61 ± 1.9	130 ± 3.6***	1.9 ± 0.11†††	17 ± 2.4**	0.64–2.8[a]
WIN55,212–2	100 ± 3.2	130 ± 4.9**	1.1 ± 0.035	−3.4 ± 3.2	0.28–16.2[a]
AM1241	100 ± 6.6	100 ± 3.5	1.0 ± 0.056	−0.83 ± 1.1	3.4[b]
JWH015	91 ± 5.8	120 ± 2.4***	1.1 ± 0.030	−3.9 ± 2.1*	14–430[a]
JWH133	77 ± 3.3	120 ± 2.7***	1.2 ± 0.058†††	18 ± 6.2*	3.4[a]
THC	100 ± 2.0	120 ± 2.2***	1.1 ± 0.058	−7.0 ± 2.7	1.7–75[a]
THCV	88 ± 2.0	120 ± 2.1**	1.0 ± 0.032	−17 ± 7.4	63–75[c]
AM1710	71 ± 3.0	120 ± 3.2**	1.3 ± 0.060†††	−3.1 ± 4.1	6.7[d]
A-836339	82 ± 2.1	120 ± 2.5***	1.2 ± 0.039††	16 ± 4.1	0.64[e]
2-AG	81 ± 6.3	130 ± 8.1*	1.1 ± 0.025	33 ± 6.2*	140–1400[a]
GW405833	N.D.	N.D.	N.D.	−2.5 ± 1.4	12[f]
AM630	100 ± 2.1	97 ± 1.3	1.0 ± 0.022	−12 ± 2.4**	31[a]
SR144528	130 ± 4.5	99 ± 2.0	0.93 ± 0.039	−10 ± 3.2*	0.040–15[a]

N.D., no data (GW405833 not tested in control cells).
* $p < 0.05$ versus untransfected control cells.
** $p < 0.01$ versus untransfected control cells.
*** $p < 0.001$ versus untransfected control cells.
†† $p < 0.01$ versus untreated control.
††† $p < 0.001$, versus untreated control.
[a] Miller and Stella, 2008.
[b] Ibrahim et al., 2003.
[c] Thomas et al., 2005.
[d] Khanolkar et al., 2007.
[e] Yao et al., 2009.
[f] Gallant et al., 1996.

zoyl)-5-methoxy-2-methyl-3-[2-(4-morpholinyl)ethyl]-1*H*-indole (GW405833) produced CB_2-dependent behavioral effects when infused into the nucleus accumbens (Xi et al., 2011), we also tested this compound to determine whether its actions could be mediated by inhibition of VGCCs. GW405833 did not produce substantial inhibition of VGCCs (Table 1). These data further suggest that CB_2 is indeed able to couple to VGCCs and that this coupling is highly ligand-dependent.

Discussion

We began this study focusing on internalization of CB_2 receptors. From our data, we conclude that different classes of cannabinoid ligands differ substantially in their ability to promote CB_2 receptor internalization. Nonclassic cannabinoids such as CP55,940 and CP47,497-C8 [a synthetic cannabinoid found in "Spice" (Atwood et al., 2011)] are the most efficacious class of cannabinoid ligands for internalization (Figs. 1 and 2; Supplemental Table 1). The aminoalkylindoles (WIN55,212-2, AM1241, JWH015, and JWH018) are the least effective (Figs. 1 and 2; Supplemental Table 1). It may be generalized that bicyclic cannabinoids are effective internalizers of CB_2, whereas aminoalkylindoles are poor internalizers. AM1241 was nearly ineffective as a CB_2 agonist in our other assays as well. However, the AM1241 in this study was a mixture of different stereoisomers and studied primarily on rodent CB_2 receptors. AM1241 produces diverse stereoisomer-specific effects at rodent and human CB_2 receptors (Bingham et al., 2007). The other classes of cannabinoid ligands have a range of efficacy for CB_2 internalization. THC produced no rCB_2 internalization, whereas the other classic cannabinoids tested here produced a moderate amount of internalization. HU-308, another classic cannabinoid, has also been reported to internalize CB_2 in HEK293 cells (Grimsey et al., 2011). The differences between THC and the other classic cannabinoids tested here parallel the weak ability of THC to activate CB_2 (Bayewitch et al., 1995) and the greater efficacies of the other compounds (Howlett et al., 2002; Bolognini et al., 2010). The same may be said of the inability of AEA to produce rCB_2 internalization, even in the presence of FAAH inhibitors. AEA is a weak partial agonist at CB_2 in many signaling pathways (Bayewitch et al., 1995). The lack of increased internalization after inhibition of MGL in both rCB_1 and rCB_2 cells suggests either that 2-AG degradation is not responsible for its low potency or that 2-AG metabolism in HEK293 cells may be mediated by hydrolases such as α/β-hydrolases 6 or 12 (Blankman et al., 2007) rather than by MGL. Supporting this latter hypothesis, microarray analysis indicates that HEK293 cells possess significant levels of α/β-hydrolase 6 and 12 mRNA but not MGL mRNA (Supplemental Table 5).

We were surprised that WIN55,212-2 did not produce receptor internalization. WIN55,212-2 is frequently used as a CB_2 receptor agonist. For example, WIN55,212-2 inhibits forskolin-stimulated cAMP accumulation in cannabinoid receptor-expressing HEK293 cells, where it is equally efficacious at CB_2 and CB_1 but is 10-fold less potent at CB_2 (Tao and Abood, 1998). We expected that, because WIN55,212-2 robustly internalizes CB_1 (Hsieh et al., 1999; Atwood et al., 2010, 2011) and is reported as an efficacious agonist at CB_2 (Howlett et al., 2002), it too would promote significant CB_2 receptor internalization. WIN55,212-2 not only failed to internalize CB_2 but also competitively antagonized internalization by CP55,940. Nonetheless, WIN55,212-2 still activated

CB_2, as evidenced by its effects on ERK1/2 and β-arrestin$_2$. Our data are consistent with previous studies that found no inhibition of VGCCs by WIN55,212-2 (Felder et al., 1995; Ross et al., 2001). In contrast, CP55,940 inhibited VGCCs (Fig. 6). Similar to results of the internalization assays (Fig. 3), WIN55,212-2 also antagonized inhibition of VGCCs by CP55,940 (Fig. 6F). The data from Fig. 6 clearly indicate that CB_2 will inhibit VGCCs, but that WIN55,212-2 does not activate CB_2 receptors in an appropriate fashion to elicit inhibition. The results reported here examining the effects of WIN55,212-2 on CB_2 receptor internalization, ERK1/2, β-arrestin, and VGCCs imply that WIN55,212-2 shows marked functionally selectivity at CB_2, whereas CP55,940 is less selective.

Functional selectivity (also known as "biased agonism" and "ligand-directed trafficking") is the pharmacological concept that agonists for a particular receptor may selectively and differentially activate specific downstream signaling pathways (Urban et al., 2007). A few studies have examined functional selectivity at CB_2 receptors. One examined CP55,940, 2-AG, and 2-arachidonoylglyceryl ether functional selectivity using MAPK activation, stimulation of calcium transients, and inhibition of adenylyl cyclase as the signaling pathways (Shoemaker et al., 2005). Each ligand differed in its rank order of potency in the three assays despite similar efficacies. Schuehly et al. (2011) recently described a case of functional selectivity of CB_2 ligands. AM630 displayed inverse agonist/antagonist actions on CB_2-mediated inhibition of cAMP production and was silent in its effects on intracellular calcium transients. On the other hand, a novel CB_2 ligand, 4′-*O*-methylhonokiol, was an inverse agonist/antagonist with regard to cAMP production but potentiated the effects of 2-AG on calcium transients. Our data extend these findings, demonstrating that specific CB_2 ligands activate a limited repertoire of signaling pathways. CP55,940 is a broad "agonist" in the classic sense, in that it is highly efficacious across all cellular signaling pathways studied here. SR144528 behaved as an inverse agonist in the internalization assays, increasing surface levels, whereas AM630 did not, behaving as a neutral antagonist (Fig. 2E$_2$; Supplemental Table 1). In other assays, these two ligands act similarly (Table 1). These observations emphasize that the concept of functional selectivity also applies to inverse agonists, in that both compounds are similarly effective inverse agonists in guanosine 5′-*O*-(3-thio)triphosphate binding assays (Ross et al., 1999). These data also support the differences (Schuehly et al., 2011) observed between SR144528 and AM630. However, the lack of effect of AM630 on CB_2 surface levels seems to contradict the Grimsey et al. (2011) report, for unclear reasons. Other ligands also displayed functional selectivity in the different signaling pathways studied here. For example, AM1710 robustly internalized CB_2 and recruited β-arrestin$_2$ but weakly activated MAPK and did not affect VGCC.

Our results provide strong evidence for functional selectivity with respect to internalization among diverse CB_2 receptor agonists. The internalization data presented here are consistent with results from other receptors, such as μ-opioid receptors, which have high and low internalizing agonists (Whistler et al., 1999; Koch and Höllt, 2008). Internalization and desensitization of CB_1 seem to be inversely correlated (Wu et al., 2008). If this holds true for CB_2, we hypothesize that WIN55,212-2 and other aminoalkylindoles will rapidly desensitize CB_2, because they produce little receptor internalization. In contrast, agonists that promote CB_2 internalization may cause less desensitization. These data may allow for the development of clinically useful, slowly desensitizing CB_2 agonists.

Rat CB_2 and mouse CB_2 can respond differently compared with human CB_2 to the same ligands (Bingham et al., 2007); thus, it was important to determine whether the results were specific to rat CB_2. Additional data suggest that WIN55,212-2, JWH015, 2-AG, and AEA are more human-preferring ligands, whereas CP55,940 shows less selectivity (Mukherjee et al., 2004). There are also two isoforms of rCB_2, one short—similar to mouse and human CB_2 (Griffin et al., 2000)—and one long (Brown et al., 2002). The studies here used the latter. On the basis of the data in Supplemental Table 3, agonist differences are much more marked than species differences. In addition, the cellular environment in which the receptor is expressed does not seem to determine the pharmacological pattern of internalization we observed, although exceptions may exist for other signaling pathways (Aramori et al., 1997). We expect that CP55,940 and WIN55,212-2 will display similar functional selectivity in cells in which CB_2 is natively expressed, although this remains to be determined.

Our results have significant implications for drug development as well as the design and interpretation of experiments studying pharmacological responses to CB_2 agonists. CB_2 agonists show substantial efficacy in multiple preclinical models, including models examining analgesia, inflammation, neuroprotection, anxiety, and ischemia/reperfusion injury. To date, however, the translation of these studies to effective CB_2-based therapeutics has been disappointing. It will be interesting to determine whether CB_2 agonist efficacy in a specific preclinical model comes with a characteristic signaling "fingerprint. " If so, the development of CB_2 agonists activating only those signaling pathways may result in efficacious drugs with fewer side effects. Functional selectivity has been demonstrated in vivo for 5HT2A as well as the opioid receptor ligands (Pradhan et al., 2011). It will be of great interest to determine whether the functionally selective CB_2 ligands identified here differ in their behavioral effects. Functional selectivity must also be considered when interpreting experiments examining CB_2 signaling. For example, WIN55,212-2 is often used as a ligand to test involvement of CB_2 in a particular pathway. If WIN55,212-2 does not activate this pathway well (e.g., VGCCs or receptor internalization), then false conclusions might be drawn on CB_2 involvement. Indeed, WIN55,212-2 may even antagonize the action of endogenous CB_2 ligands, such as 2-AG, further confounding interpretation. As Table 1 indicates, CB_2 ligands differ greatly in their activation of specific signaling pathways. This mandates caution in the interpretation of CB_2 signaling studies that employ only one cannabinoid as the ligand. More broadly, it encourages careful consideration of data that use a single ligand as pharmacological "proof" of the role (or not) of CB_2 in a physiological process. The pronounced functional selectivity of CB_2 ligands we have characterized in this study opens promising new avenues for drug discovery and for understanding the varied physiological roles of the CB_2 receptor.

Acknowledgments

We thank Douglas McHugh for help in optimizing the MAPK assay, Natasha Murataeva for help with data collection, Odile El Kouhen at Abbott Laboratories for assistance in obtaining A-836339 and for comments on an earlier version of the manuscript, and Gerry Oxford for AtT20 cells and helpful discussions on their use. We also thank Andrea Hohmann and Alex Makriyannis for the gift of AM1710, John Huffman for the gift of JWH018, Aron Lichtman for the gift of THCV, and Raphael Mechoulam for the gift of HU210.

Authorship Contributions

Participated in research design: Atwood, Straiker, and Mackie.

Conducted experiments: Atwood, Wager-Miller, Haskins, and Straiker.

Performed data analysis: Atwood, Wager-Miller, and Straiker.

Wrote or contributed to the writing of the manuscript: Atwood, Straiker, Mackie, and Wager-Miller.

References

Anand P, Whiteside G, Fowler CJ, and Hohmann AG (2009) Targeting CB2 receptors and the endocannabinoid system for the treatment of pain. *Brain Res Rev* **60:**255–266.

Aramori I, Ferguson SS, Bieniasz PD, Zhang J, Cullen B, and Cullen MG (1997) Molecular mechanism of desensitization of the chemokine receptor CCR-5: receptor signaling and internalization are dissociable from its role as an HIV-1 coreceptor. *EMBO J* **16:**4606–4616.

Atwood BK, Huffman J, Straiker A, and Mackie K (2010) JWH018, a common constituent of 'Spice' herbal blends, is a potent and efficacious cannabinoid CB receptor agonist. *Br J Pharmacol* **160:**585–593.

Atwood BK, Lee D, Straiker A, Widlanski TS, and Mackie K (2011) CP47,497-C8 and JWH073, commonly found in 'Spice' herbal blends, are potent and efficacious CB1 cannabinoid receptor agonists. *Eur J Pharmacol* **659:**139–145.

Atwood BK and Mackie K (2010) CB2: a cannabinoid receptor with an identity crisis. *Br J Pharmacol* **160:**467–479.

Bayewitch M, Avidor-Reiss T, Levy R, Barg J, Mechoulam R, and Vogel Z (1995) The peripheral cannabinoid receptor: adenylate cyclase inhibition and G protein coupling. *FEBS Lett* **375:**143–147.

Benito C, Kim WK, Kim WK, Chavarría I, Hillard CJ, Mackie K, Tolón RM, Williams K, Williams K, and Romero J (2005) A glial endogenous cannabinoid system is upregulated in the brains of macaques with simian immunodeficiency virus-induced encephalitis. *J Neurosci* **25:**2530–2536.

Berdyshev EV (2000) Cannabinoid receptors and the regulation of immune response. *Chem Phys Lipids* **108:**169–190.

Bingham B, Jones PG, Uveges AJ, Kotnis S, Lu P, Smith VA, Sun SC, Resnick L, Chlenov M, He Y, et al. (2007) Species-specific in vitro pharmacological effects of the cannabinoid receptor 2 (CB2) selective ligand AM1241 and its resolved enantiomers. *Br J Pharmacol* **151:**1061–1070.

Blankman JL, Simon GM, and Cravatt BF (2007) A comprehensive profile of brain enzymes that hydrolyze the endocannabinoid 2-arachidonoylglycerol. *Chem Biol* **14:**1347–1356.

Bolognini D, Costa B, Maione S, Comelli F, Marini P, Di Marzo V, Parolaro D, Ross RA, Gauson LA, Cascio MG, et al. (2010) The plant cannabinoid Delta9-tetrahydrocannabivarin can decrease signs of inflammation and inflammatory pain in mice. *Br J Pharmacol* **160:**677–687.

Bouaboula M, Dussossoy D, and Casellas P (1999) Regulation of peripheral cannabinoid receptor CB2 phosphorylation by the inverse agonist SR 144528. Implications for receptor biological responses. *J Biol Chem* **274:**20397–20405.

Brown SM, Wager-Miller J, and Mackie K (2002) Cloning and molecular characterization of the rat CB2 cannabinoid receptor. *Biochim Biophys Acta* **1576:**255–264.

Cabral GA and Griffin-Thomas L (2009) Emerging role of the cannabinoid receptor CB2 in immune regulation: therapeutic prospects for neuroinflammation. *Expert Rev Mol Med* **11:**e3.

Cravatt BF, Demarest K, Patricelli MP, Bracey MH, Giang DK, Martin BR, and Lichtman AH (2001) Supersensitivity to anandamide and enhanced endogenous cannabinoid signaling in mice lacking fatty acid amide hydrolase. *Proc Natl Acad Sci USA* **98:**9371–9376.

Daigle TL, Kearn CS, and Mackie K (2008) Rapid CB1 cannabinoid receptor desensitization defines the time course of ERK1/2 MAP kinase signaling. *Neuropharmacology* **54:**36–44.

Felder CC, Joyce KE, Briley EM, Mansouri J, Mackie K, Blond O, Lai Y, Ma AL, and Mitchell RL (1995) Comparison of the pharmacology and signal transduction of the human cannabinoid CB1 and CB2 receptors. *Mol Pharmacol* **48:**443–450.

Finn AK and Whistler JL (2001) Endocytosis of the mu opioid receptor reduces tolerance and a cellular hallmark of opiate withdrawal. *Neuron* **32:**829–839.

Gallant M, Dufresne C, Gareau Y, Guay D, Leblanc Y, Prasit P, Rochette C, Sawyer N, Slipetz DM, Tremblay N, et al. (1996) New class of potent ligands for the human peripheral cannabinoid receptor. *Bioorg Med Chem Lett* **6:**2263–2268.

Griffin G, Tao Q, and Abood ME (2000) Cloning and pharmacological characterization of the rat CB(2) cannabinoid receptor. *J Pharmacol Exp Ther* **292:**886–894.

Grimsey NL, Goodfellow CE, Dragunow M, and Glass M (2011) Cannabinoid receptor 2 undergoes Rab5-mediated internalization and recycles via a Rab11-dependent pathway. *Biochim Biophys Acta* **1813:**1554–1560.

Howlett AC, Barth F, Bonner TI, Cabral G, Casellas P, Devane WA, Felder CC, Herkenham M, Mackie K, Martin BR, et al. (2002) International Union of Pharmacology. XXVII. Classification of cannabinoid receptors. *Pharmacol Rev* **54:**161–202.

Hsieh C, Brown S, Derleth C, and Mackie K (1999) Internalization and recycling of the CB1 cannabinoid receptor. *J Neurochem* **73:**493–501.

Huestis MA, Gorelick DA, Heishman SJ, Preston KL, Nelson RA, Moolchan ET, and Frank RA (2001) Blockade of effects of smoked marijuana by the CB1-selective cannabinoid receptor antagonist SR141716. *Arch Gen Psychiatry* **58:**322–328.

Huffman JW, Dong D, Martin BR, and Compton DR (1994) Design, Synthesis and Pharmacology of Cannabimimetic Indoles. *Bioorganic & Medicinal Chemistry Letters* **4:**563–566.

Ibrahim MM, Deng H, Zvonok A, Cockayne DA, Kwan J, Mata HP, Vanderah TW, Lai J, Porreca F, Makriyannis A, et al. (2003) Activation of CB2 cannabinoid receptors by AM1241 inhibits experimental neuropathic pain: pain inhibition by receptors not present in the CNS. *Proc Natl Acad Sci USA* **100:**10529–10533.

Kearn CS, Blake-Palmer K, Daniel E, Mackie K, and Glass M (2005) Concurrent stimulation of cannabinoid CB1 and dopamine D2 receptors enhances heterodimer formation: a mechanism for receptor cross-talk? *Mol Pharmacol* **67:**1697–1704.

Khanolkar AD, Lu D, Ibrahim M, Duclos RI Jr, Thakur GA, Malan TP Jr, Porreca F, Veerappan V, Tian X, George C, et al. (2007) Cannabilactones: a novel class of CB2 selective agonists with peripheral analgesic activity. *J Med Chem* **50:**6493–6500.

Koch T and Höllt V (2008) Role of receptor internalization in opioid tolerance and dependence. *Pharmacol Ther* **117:**199–206.

Koch T, Widera A, Bartzsch K, Schulz S, Brandenburg LO, Wundrack N, Beyer A, Grecksch G, and Höllt V (2005) Receptor endocytosis counteracts the development of opioid tolerance. *Mol Pharmacol* **67:**280–287.

Ligresti A, Cascio MG, and Di Marzo V (2005) Endocannabinoid metabolic pathways and enzymes. *Curr Drug Targets CNS Neurol Disord* **4:**615–623.

Long JZ, Li W, Booker L, Burston JJ, Kinsey SG, Schlosburg JE, Pavón FJ, Serrano AM, Selley DE, Parsons LH, et al. (2009) Selective blockade of 2-arachidonoylglycerol hydrolysis produces cannabinoid behavioral effects. *Nat Chem Biol* **5:**37–44.

Mackie K (2005) Distribution of cannabinoid receptors in the central and peripheral nervous system. *Handb Exp Pharmacol* **168:**299–325.

Miller AM and Stella N (2008) CB2 receptor-mediated migration of immune cells: it can go either way. *Br J Pharmacol* **153:**299–308.

Monory K, Blaudzun H, Massa F, Kaiser N, Lemberger T, Schütz G, Wotjak CT, Lutz B, and Marsicano G (2007) Genetic dissection of behavioural and autonomic effects of Delta(9)-tetrahydrocannabinol in mice. *PLoS Biol* **5:**e269.

Mukherjee S, Adams M, Whiteaker K, Daza A, Kage K, Cassar S, Meyer M, and Yao BB (2004) Species comparison and pharmacological characterization of rat and human CB2 cannabinoid receptors. *Eur J Pharmacol* **505:**1–9.

Pradhan AA, Befort K, Nozaki C, Gavériaux-Ruff C, and Kieffer BL (2011) The delta opioid receptor: an evolving target for the treatment of brain disorders. *Trends Pharmacol Sci* **32:**581–590.

Rahn EJ, Thakur GA, Wood JA, Zvonok AM, Makriyannis A, and Hohmann AG (2011) Pharmacological characterization of AM1710, a putative cannabinoid CB2 agonist from the cannabilactone class: antinociception without central nervous system side-effects. *Pharmacol Biochem Behav* **98:**493–502.

Rajagopal S, Rajagopal K, and Lefkowitz RJ (2010) Teaching old receptors new tricks: biasing seven-transmembrane receptors. *Nat Rev Drug Discov* **9:**373–386.

Ross RA, Brockie HC, Stevenson LA, Murphy VL, Templeton F, Makriyannis A, and Pertwee RG (1999) Agonist-inverse agonist characterization at CB1 and CB2 cannabinoid receptors of L759633, L759656, and AM630. *Br J Pharmacol* **126:**665–672.

Ross RA, Coutts AA, McFarlane SM, Anavi-Goffer S, Irving AJ, Pertwee RG, MacEwan DJ, and Scott RH (2001) Actions of cannabinoid receptor ligands on rat cultured sensory neurones: implications for antinociception. *Neuropharmacology* **40:**221–232.

Schuehly W, Paredes JM, Kleyer J, Huefner A, Anavi-Goffer S, Raduner S, Altmann KH, and Gertsch J (2011) Mechanisms of osteoclastogenesis inhibition by a novel class of biphenyl-type cannabinoid CB(2) receptor inverse agonists. *Chem Biol* **18:**1053–1064.

Shoemaker JL, Ruckle MB, Mayeux PR, and Prather PL (2005) Agonist-directed trafficking of response by endocannabinoids acting at CB2 receptors. *J Pharmacol Exp Ther* **315:**828–838.

Tao Q and Abood ME (1998) Mutation of a highly conserved aspartate residue in the second transmembrane domain of the cannabinoid receptors, CB1 and CB2, disrupts G-protein coupling. *J Pharmacol Exp Ther* **285:**651–658.

Thomas A, Stevenson LA, Wease KN, Price MR, Baillie G, Ross RA, and Pertwee RG (2005) Evidence that the plant cannabinoid Delta9-tetrahydrocannabivarin is a cannabinoid CB1 and CB2 receptor antagonist. *Br J Pharmacol* **146:**917–926.

Urban JD, Clarke WP, von Zastrow M, Nichols DE, Kobilka B, Weinstein H, Javitch JA, Roth BL, Christopoulos A, Sexton PM, et al. (2007) Functional selectivity and classical concepts of quantitative pharmacology. *J Pharmacol Exp Ther* **320:**1–13.

von Zastrow M, Svingos A, Haberstock-Debic H, and Evans C (2003) Regulated endocytosis of opioid receptors: cellular mechanisms and proposed roles in physiological adaptation to opiate drugs. *Curr Opin Neurobiol* **13:**348–353.

Whistler JL, Chuang HH, Chu P, Jan LY, and von Zastrow M (1999) Functional dissociation of mu opioid receptor signaling and endocytosis: implications for the biology of opiate tolerance and addiction. *Neuron* **23:**737–746.

Wotherspoon G, Fox A, McIntyre P, Colley S, Bevan S, and Winter J (2005) Peripheral nerve injury induces cannabinoid receptor 2 protein expression in rat sensory neurons. *Neuroscience* **135:**235–245.

Wu DF, Yang LQ, Goschke A, Stumm R, Brandenburg LO, Liang YJ, Höllt V, and Koch T (2008) Role of receptor internalization in the agonist-induced desensitization of cannabinoid type 1 receptors. *J Neurochem* **104:**1132–1143.

Xi ZX, Peng XQ, Li X, Song R, Zhang HY, Liu QR, Yang HJ, Bi GH, Li J, and Gardner

EL (2011) Brain cannabinoid CB(2) receptors modulate cocaine's actions in mice. *Nat Neurosci* **14:**1160–1166.
Yao BB, Hsieh G, Daza AV, Fan Y, Grayson GK, Garrison TR, El Kouhen O, Hooker BA, Pai M, Wensink EJ, et al. (2009) Characterization of a cannabinoid CB2 receptor-selective agonist, A-836339 [2,2,3,3-tetramethyl-cyclopropanecarboxylic acid [3-(2-methoxy-ethyl)-4,5-dimethyl-3H-thiazol-(2Z)-ylidene]-amide], using in vitro pharmacological assays, in vivo pain models, and pharmacological magnetic resonance imaging. *J Pharmacol Exp Ther* **328:**141–151.
Yiangou Y, Facer P, Durrenberger P, Chessell IP, Naylor A, Bountra C, Banati RR, and Anand P (2006) COX-2, CB2 and P2X7-immunoreactivities are increased in activated microglial cells/macrophages of multiple sclerosis and amyotrophic lateral sclerosis spinal cord. *BMC Neurol* **6:**12.
Zhang J, Hoffert C, Vu HK, Groblewski T, Ahmad S, and O'Donnell D (2003) Induction of CB2 receptor expression in the rat spinal cord of neuropathic but not inflammatory chronic pain models. *Eur J Neurosci* **17:**2750–2754.

Address correspondence to: Ken Mackie, Department of Psychological and Brain Sciences, Indiana University, 1101 E. 10th Street, Bloomington, IN 47405. E-mail: kmackie@indiana.edu